AERODYNAMIC INSTABILITY OF SUPERSONIC INTAKE DIFFUSERS

by

T. Yoshinaka

A RESEARCH THESIS

IN THE

FACULTY OF ENGINEERING

Presented in partial fulfilment of the requirements for the

Degree of MASTER OF ENGINEERING

at

Sir George Williams University

Montreal, Canada

15 August 1970

Name of Author: T. Yoshinaka

Title of Thesis: Aerodynamic Instability of Supersonic Intake Diffusers

ABSTRACT

The instability of the shock wave in front of a supersonic intake diffuser is theoretically analyzed in this report. From a critical review of the previous investigations, it has been obtained that a reduction of the effective flow area at the diffuser inlet is essential to starting the low frequency oscillation, the buzz.

A theoretical analysis of an interaction between an isentropic disturbance and a normal shock wave indicates that an upstream rarefaction wave of the shock and a downstream compression wave can have the potential to initiate the buzz. Simple mathematical formulae of the plenum pressure during the discharge and the fill-up periods of the buzz cycle have been developed in this report.

A theory of the high frequency oscillation, the organ pipe oscillation, is presented. This theory was obtained using the technique developed by D.S. Whitehead. It has been found that the frequency increases with decreasing the flow Mach number of the diffuser and coincides with the typical organ pipe frequency when the flow Mach number is zero. This high frequency oscillation has a positive damping characteristic.

ACKNOWLEDGEMENTS

The author wishes to express his appreciation to his supervisor, Dr.C.C.K. Kwok, for his encouragement and guidance throughout all stages of this work.

Special thanks are extended to Dr. Sui Lin and Dr. T. Sankar for their numerous constructive criticisms and discussions.

The author is also grateful to Miss Nancy de St.Croix for correcting and typing the manuscript.

The financial support of the United Aircraft of Canada Limited and the National Research Council of Canada under grant number A7435 are gratefully acknowledged.

SUMMARY

The aerodynamic instability of supersonic intake diffusers is investigated theoretically in this report. The instability is divided into two parts. One is called the low frequency oscillation or the buzz, and the other is called the high frequency oscillation or the organ pipe oscillation. A possible buzz initiation mechanism is analyzed and a theory for the plenum pressure during the buzz is developed. The characteristics of the organ pipe oscillation are also presented and discussed.

TABLE OF CONTENTS

TABLE OF CONTENTS (cont'd)

LIST OF SYMBOLS

Notations

A	Flow area
a	Acoustic velocity
C_1, C_2, C_3, C_4	Constants (see Eqn.(3.1-65), Eqn.(3.1-71))
C_p	Specific heat with constant pressure
C_v	Specific heat with constant volume
F,f	Arbitrary functions of $(x - a_o t)$ (see Eqn.(3.1-24), Eqn.(3.1-25))
f	Frequency of oscillation
G,g	Arbitrary functions of $(x + a_o t)$ (see Eqn.(3.1-24), Eqn.(3.1-25))
g	Gravitational acceleration
J	Mechanical equivalent of heat
K	Constant (see Eqn.(3.1-65))
l	Axial length of diffuser or plenum chamber
m	Mass flow rate
n	Mode of oscillation
P_t	Total pressure
p	Static pressure
R	Coefficient of reflection (see Eqn.(3.1-50))
R	Universal gas constant

LIST OF SYMBOLS (cont'd)

s	Entropy
$\tilde{s}$	Condensation (see Eqn.(3.1-17))
T	Transmission coefficient (see Eqn.(3.1-39))
T	Temperature
t	Time
u	Flow velocity
V	Volume of plenum chamber
x	Axial coordinate (see Fig.4)
α	Constant (defined in Eqn.(3.2-3))
$\gamma=c_p/c_v$	Ratio of specific heat (=1.4 for air)
δ	Logarithmic decrement of amplitude (see Eqn.(3.2-23))
ν	Function of x defined in Eqn.(3.2-3)
ξ	Perturbed shock velocity
ρ	Density
σ	Function of x defined in Eqn.(3.2-3)
$\omega=2\pi f$	Angular frequency

Superscripts

$-$	Average
$'$	Perturbation propagated downstream
$''$	Perturbation propagated upstream
$*$	Critical condition, i.e. M=1

LIST OF SYMBOLS (cont'd)

Subscripts

f	Initial condition of the fill-up period in the buzz cycle
i	Initial condition of the discharge period in the buzz cycle
t	Stagnation
0,1,2,3,4, 41,42,5	Locations defined in Figs.1 and 4

1. INTRODUCTION

1.1 GENERAL

Nowadays, supersonic aircraft are becoming popular in the military service. Also in the civil aviation field, two of the supersonic transports, the Anglo-French "Concord" and the Russian "TU-144" are on the stage of flight testing. This increase in flight velocity however, requires many aerodynamic and mechanical problems to be solved. One aerodynamic problem is to design a high performance air intake diffuser for the jet engine. Although the flight speed varies from zero to a supersonic speed, all available jet engines in the present days necessitate that the flow be subsonic at the compressor inlet. Therefore, the flow must be diffused from the supersonic flight speed to a subsonic speed which meets the engine requirements.

A diffusion of the supersonic airflow is usually associated with a single or multiple shock waves and significant pressure losses are expected when the air flow passes across the shocks. A magnitude of the loss is a function of the upstream Mach number, the shock pattern (whether it is normal or oblique) and the intake geometry. One of the serious problems is the fact that the shock becomes unstable under a certain operating condition. This shock instability sometimes results in a periodical

compressor surge and a flame-out, subsequently leading to mechanical failure of the engine. Although this is a very serious problem for the supersonic vehicles, an accurate and complete mechanism of the shock instability phenomena is not fully understood.

The purpose of this report is to analyze this flow instability problem theoretically, taking into consideration the results of a number of previous investigations. In the first part of this report, the diffuser characteristics at the steady state operating condition are discussed in order to understand the condition in which the instability phenomena occur. A physical explanation of the unstable operating condition is presented in the second part, based mainly on the experimental results obtained from previous investigators. A discussion of several theories proposed by the investigators on this problem is also presented. Finally, the flow instability is critically analyzed and discussed in an attempt to acquire a better understanding of this highly complex phenomenon.

1.2 STEADY STATE OPERATING CONDITION

Consider a supersonic intake diffuser as shown in Fig. 1. If the flow is assumed to be quasi-one-dimensional and inviscid, the mass flow rate, m, can be expressed by the following formula:

$$m = \rho A u = pAM\sqrt{\frac{\gamma g}{RT}} = \frac{P_t}{\sqrt{T_t}} A M \frac{p}{P_t}\sqrt{\frac{\gamma g}{R}\frac{T_t}{T}}$$

$$= \frac{P_t}{\sqrt{T_t}} A\sqrt{\frac{\gamma g}{R}} M\left(1+\frac{\gamma-1}{2}M^2\right)^{\frac{1}{2}-\frac{\gamma}{\gamma-1}}$$

$$= \frac{P_t}{\sqrt{T_t}} A\frac{\gamma\sqrt{g}}{\sqrt{JC_p(\gamma-1)}} M\left(1+\frac{\gamma-1}{2}M^2\right)^{-\frac{(\gamma+1)}{2(\gamma-1)}}$$

$$= \frac{P_t}{\sqrt{T_t}} A\sqrt{\frac{g}{JC_p}} F(M) \qquad (1\text{-}1)$$

where, $F(M) = \frac{\gamma}{\sqrt{\gamma-1}} M\left(1+\frac{\gamma-1}{2}M^2\right)^{-\frac{(\gamma+1)}{2(\gamma-1)}}$ is called the Fliegner's number. Since the mass conservation holds between Station 0 and Station 4 (see Fig. 1),

$$m_0 = \frac{P_{t_0}}{\sqrt{T_{t_0}}} A_0\sqrt{\frac{g}{JC_p}} F(M_0) = m_4 = \frac{P_{t_4}}{\sqrt{T_{t_4}}} A_4\sqrt{\frac{g}{JC_p}} F(M_4) \qquad (1\text{-}2)$$

Assuming that the flow process between Station 0 and Station 4 is adiabatic, then neither work nor heat is added to or extracted from the outer boundary,

$$T_{t_0} = T_{t_4}$$

Therefore, from Eqn.(1-2),

$$\frac{P_{t_4}}{P_{t_0}} = \frac{A_0}{A_4}\frac{F(M_0)}{F(M_4)} \qquad (1\text{-}3)$$

where, C_p is assumed to be constant.

Considering the imaginary sonic points for the flow at Station 0 and Station 4, as shown in Fig. 2, the following relationship can be obtained:

$$\frac{P_{t4}^*}{P_{t0}^*} = \frac{P_{t4}}{P_{t0}} = \frac{A_0^*}{A_4^*}\frac{F(1)}{F(1)} = \frac{A_0^*}{A_4^*} \qquad (1\text{-}4)$$

where, a superscript,*, represents the sonic condition. Eqn.(1-4) can be rewritten with the mass flow rate,m, as shown below:

$$\frac{P_{t4}}{P_{t0}} = \frac{A_0^*}{A_4^*} = \frac{m_0}{m_{0c}}\frac{m_{0c}}{m_0}\frac{A_0^*}{A_4^*} = \frac{m_0}{m_{0c}}\frac{A_{0c}}{A_4}\frac{A_4}{A_0}\frac{A_0^*}{A_4^*}$$

$$= \frac{m_0}{m_{0c}}\left(\frac{A_{0c}}{A_4}\right)\left(A_0^*/A_0\right)/\left(A_4^*/A_4\right) \qquad (1\text{-}5)$$

where, a subscript,c, represents a critical condition which will be discussed in the following paragraphs. Since A_{0c} and A_4 are constant values, the pressure ratio, P_{t4}/P_{t0}, is thus directly related to the mass flow ratio, m_0/m_{0c}. $[(A_0^*/A_0)/(A_4^*/A_4)]$ is a characteristic parameter depending on the geometric configuration of the diffuser. A qualitative curve of Eqn.(1-5) is presented in Fig. 3.

When a single or multiple shocks exists somewhere at the downstream of Station 3, A_0 is independent of the shock location. This is called a "supercritical" condition (see Fig. 3A). If the flight condition and the up stream condition of the intake are unchanged, the mass flow rate is constant. However, the pressure ratio, P_{t4}/P_{t0}, decreases

if the shock moves downstream. This is because an upstream Mach number of the shock increases, resulting in higher pressure loss across the shock. If the shock moves upstream and passes by Station 3, which is considered to be the diffuser throat, the shock jumps to the inlet lip, since the shock is inherently unstable in a convergent section of a duct. When the shock reaches the inlet lip, the operating condition is called a "critical" condition. If the shock location is moved further upstream, the shock detaches from the inlet lip. The entering mass flow is then reduced by a spillage of the flow between the shock and the inlet lip. Since the mass flow decreases, the friction loss in the diffuser is also decreased, provided a triple point of the shock is kept in the outside of the stagnation stream line as shown in Fig. 3B. This condition is called "high-subcritical" condition. With the reduction of friction loss in the diffuser at the high-subcritical condition, the pressure ratio is slightly higher than that at the critical condition. A further movement of the shock location causes the shock to encounter the free stream directly as shown in Fig. 3C. Since the pressure loss across a single normal shock is higher than that across an oblique shock followed by a normal shock, the total pressure ratio P_{t4}/P_{t_0}, decreases while decreasing the mass flow rate. This condition is called a "low subcritical" condition. The pressure ratio, P_{t4}/P_{t_0}, approaches a value between 0 and 1 when the mass flow

reduces to 0. From experimental observation, it was confirmed that the moving shock is single at the critical and subcritical conditions irrespective of whether the shock is single or multiple at the supercritical condition.

In order to understand the change in diffuser characteristics with changes in diffuser geometry while operating at the steady state condition, it is much simpler to consider an open nose intake diffuser as shown in Fig. 4. The location of the stations corresponds to those of the spike diffuser (see Fig. 3). For the open nose diffuser, there is no oblique shock ahead of the inlet lip. Therefore the Mach number of the open nose diffuser is always higher at the inlet lip (Station 2) than that of the spike diffuser. As a result, in the super critical condition, the open nose diffuser has a higher loss. The pressure ratio at the critical condition (point A in Fig. 3) of the open nose diffuser is slightly lower than that of the spike diffuser. When the shock of the open nose diffuser is at the inlet lip, the upstream Mach number is actually the flight Mach number. Therefore, a further movement of the shock in the upstream direction decreases the difference in the pressure ratio, P_{t4}/P_{t0}, between the spike and open nose diffusers. When the mass flow approaches zero, the shock pattern in both diffusers is the same. Therefore, both diffusers have the same pressure ratio at zero mass flow condition.

The flow instability occurs only in the subcritical condition. This flow instability is composed of two different phenomena. One is called a "buzz", during which the pressure and velocity in the diffuser fluctuate periodically with a relatively low frequency. The magnitude of the fluctuation is high enough for the engine compressor and the combustion chamber to suffer from the periodical surge and flame-out. Several experimental results from Ref. 1 indicate that if the compressor surge and the flame-out occur, it will be during the first "buzz" cycle. There is another flow fluctuation in which frequency is higher than that of the "buzz". This appears at a very low mass flow condition and during the "buzz" cycle. Since this high frequency oscillation apparently coincides with several times the fundamental mode of the diffuser natural frequency, this is usually called an "organ pipe oscillation". This high frequency oscillation generally has less effect on the engine performance than the "buzz".

1.3 LOW FREQUENCY OSCILLATION

As stated in the previous section, the buzz phenomenon occurs under the subcritical operating condition. According to the test results of a model and a full size engine (Ref. 1, Ref. 2, etc.), a sequence of the buzz phenomenon is as follows:

1. The shock positioned outside and near the inlet lip (Cond. A in Fig. 5) moves upstream abruptly. The forward movement of the shock results in an excessive mass spillage between the shock and the inlet lip. The static pressure in the diffuser decreases sharply in this condition (Cond. B).

2. The shock reduces and rests at a certain location infront of the inlet lip accompanied by the high frequency oscillation (Cond. C). The compressor surge and the flame-out begin at Cond. B or Cond. C.

3. The shock starts moving downstream with much lower speed than its forward movement. The high frequency oscillation still remains in this condition. The pressure in the diffuser remains constant or decreases gradually (Cond. D).

4. Finally, the shock attaches to the inlet lip and is swallowed into the diffuser (Cond. E). At this condition, the mass flow rate into the intake is maximum.

5. The shock moves further downstream. The mass flow rate is still maximum. Since the pressure loss is low if the shock is located near the inlet lip, the static pressure in the diffuser increases steeply at the first moment of this condition (Cond. F). The shock reaches its downstream dead end point and is moved back again in the upstream direction, resulting from the increasing downstream static pressure of the shock. The surge and flame-out disappear in this condition. Finally, the shock arrives at the initial location (Cond. A), completing one buzz cycle.

Fig. 5 was obtained from the experimental data of Ref. 1; however, these characteristics on the shock location and pressure history are quite consistant in any other experimental data (for example, Refs. 2 and 3).

1.4 HIGH FREQUENCY OSCILLATION

The high frequency oscillation reported in Refs. 1, 2 and 4 is observed at a very low mass flow (or the zero mass flow condition) and during each buzz cycle. Since this frequency apparently coincides with several times the diffuser natural frequency, $f=(\frac{n}{2}-\frac{1}{4})\frac{a}{\ell}$ (where n=1,2,..., a=velocity of sound and ℓ=axial length of the intake diffuser), this is called the "organ pipe" oscillation. Depending on the diffuser geometry, especially the diffuser length, and an amount of the mass flow, the value, n, varies.

2. REVIEW OF PREVIOUS INVESTIGATIONS

2.1 LOW FREQUENCY OSCILLATION

First mention of this flow instability phenomenon was made by K. Oswatitsch in 1944 (Ref. 5), translated into English and published as NACA TM 1140 in 1947. Although Oswatitsch recognized this phenomenon during his testing and observed a process of the buzz cycle experimentally with the spark pictures, he did not investigate deeply because he believed that this condition was to be avoided during the normal engine operating condition.

Pearce (Ref. 6) investigated the same problem and concluded that the positive gradient of the characteristic curve (for example, Fig. 3) has an important effect on the low frequency oscillation, the buzz. If the positive gradient of the characteristic curve is "sufficiently steep", the flow becomes unstable, but if not, the flow becomes stable. It can be said that his analysis is similar to the stability criterion of a compressor. However, it should be noted that the slope itself is a test result and therefore represents a sufficient condition for the instability. Pearce, however, did not explain the basic mechanism of the buzz.

Ferri and Nucci (Ref. 7) tested a supersonic intake with a center body, similar to an intake diffuser shown in Fig. 1. They showed that an effective area reduction at the

diffuser inlet lip due to a single vortex sheet originated at the triple point of the shock (see Fig. 6) initiated the buzz. The flow which passes across two shocks, AE and AD (see Fig. 6) has a different total pressure from the flow which crosses the single shock, AB. Following the shock, both flows keep touching each other on a plane called the contact surface. Across the contact surface, both flows have the same flow direction and the same static pressure, with only the flow velocity different. This results in generating the vortex sheet on the contact surface. If the shock moves upstream, the triple point A comes down closer to the point D. Eventually, there must be a condition in which the vortex sheet is swallowed in the intake. According to Ferri and Nucci, this swallowed vortex sheet touches the inlet cowl inner wall (see Fig. 6B), causing the flow separation and therefore a reduction of an effective flow area at the diffuser inlet lip. This phenomenon initiates the buzz. When the flow area is reduced, the expelled mass flow between the shock and the inlet lip increases. If the shock moves further upstream, the vortex sheet moves towards the inner body. As this happens, the vortex sheet detaches from the inner wall of the inlet cowl, and the separated flow on the wall re-attaches. This leads to an increase in mass flow (see Fig. 6C), and the shock then starts to move downstream. When the shock moves back allowing the vortex sheet to touch with the inner wall of the inlet cowl, the flow

separation occurs again, thus the buzz cycle repeats.

The same phenomenon appears if the separation occurs on the surface of the center body. When this separation occurs, a lambda-type shock appears (see Fig. 7). Therefore, a vortex sheet is generated from point A, and the buzz cycle may start in the same manner as stated above.

The above mentioned theory seems to be in good agreement with Ferri and Nucci's test results. However, as pointed out by Trimpi (Refs. 3 and 4) and confirmed by Dailey (Ref. 1), the swallowing of the vortex sheet is not always a necessary condition, since the buzz could occur without the vortex sheet in the diffuser. An important fact is that enough reduction of the effective flow area at the inlet lip must be obtained to start the buzz. Therefore, if the effect of the vortex sheet on the flow at the inner wall of the inlet cowl is small, the buzz does not start even if the vortex sheet is swallowed and tries to separate the flow on the inner wall of the inlet cowl. On the other hand, if the flow separation on the center body is strong enough to considerably reduce the flow area at the inlet lip, the buzz starts even if the vortex sheet does not attach to the inlet cowl inner wall.

Dailey (Ref. 1) tested a supersonic inlet similar to that of Ferri and Nucci in order to understand the buzz

mechanism by measuring the instantaneous static pressures at many locations in the intake diffuser. From many pressure recordings and a schlieren movie, he found a precise procedure of the buzz cycle. The steady high subcritical condition (see Fig. 3) is interrupted by a random pressure pulse from downstream and the shock is pushed upstream until the inlet blocks the flow. Some of the mass that enters the diffuser then begins to accumulate upstream of the blockage point. The pressure increases in this region and results in a further forward movement of the shock. This motion is unstable and is associated with the high frequency oscillation.

The mass flow entering the diffuser begins to decrease as soon as the inlet blocks, and continually decreases as the blocking progresses. The pressure downstream of the blockage point therefore begins to drop as soon as the inlet blocks. Then, the subcritical shock moves back into the diffuser and the flow enters at the supercritical rate. Because of the low plenum chamber pressure, the exit flow rate is less than the equilibrium value. Therefore, the net inflow is positive, and the plenum chamber pressure increases until the diffuser breaks down again.

Dailey concluded that the inlet blockage is caused by the flow separation on the center body. This is the only origin of the pressure pulse propagated to the shock from

downstream and triggers the buzz. Therefore, the plenum chamber pressure only reflects the history of the breakdown within the inlet and does not affect the buzz initiation.

During the buzz, Dailey noted that the mass accumulated between the blocked inlet lip and the shock. An amount of mass is expelled between the inlet lip and the shock. Then the flow streamlines must have a large curvature near the inlet lip (see Fig. 9). This results in a high static pressure on the center body near the inlet lip.

According to the pressure recording (see Fig. 8) of Dailey's test, the static pressure between the shock and the inlet lip slightly increases when the static in the plenum chamber starts decreasing. Dailey conjectured the mass accumulation from this pressure recording; however, this pressure increase is difficult to understand. If the mass were accumulated between the shock and the inlet lip, the flow velocity in the accumulated region would be very low or even zero. There would then be no possibility of flow separation on the center body. If the separation disappeared, a large amount of the flow would enter the diffuser, as long as the flow separation on the center body is the only origin of the inlet blockage, as Dailey pointed out. This is contradictory to his observation. If the blockage at the inlet lip due to the separation on the

center body progresses, the entering mass flow decreases. Therefore, this theory is only applicable to the intake diffuser with a center body. For example, in a case of an open nose diffuser, an oblique shock does not exist in front of the normal shock. Furthermore, no flow separation can occur ahead of the inlet lip.

If Dailey's theory is applied to a simple open nose intake, the blockage must be due to the boundary layer thickness or a flow separation on the diffuser wall. Therefore, the blockage occurs not at the inlet lip. but somewhere in the diffuser portion.

Considering the buzz phenomenon shown by Dailey and examining his theory carefully, one can say that Dailey's theory does not contradict Ferri and Nucci's theory. In fact, the vortex sheet of Ferri and Nucci's theory is not necessary for the flow instability. However, the flow separation at the inlet lip, due to either the vortex sheet or the steep positive pressure gradient along the flow direction, reduces the flow effective area and initiates the buzz.

Sterbentz and Evvard (Ref. 8) analyzed this problem as a sound resonator. During the buzz, the air is alternately accelerated or decelerated as the shock is swallowed and expelled. A portion of this mass flow could then act as an

internal plug resonating against the combustion chamber in a manner analogous to that of a sound resonator. They found that the frequency of the buzz oscillation can be expressed by the formula:

$$f = \frac{a}{2\pi}\sqrt{\frac{A}{V_c \cdot \ell}}$$

where, a = acoustic velocity at a point downstream of the perturbation.

A = cross sectional area of the inlet.

V_c = volume of the plenum chamber.

ℓ = diffuser length.

Sterbentz and Evvard also presented a characteristic slope, D :

$$D = d(P_{t4}/P_{t0})/d(m_4/m_{0c})$$

where, P_t = total pressure.

m = mass flow.

4 = plenum chamber.

0 = infinite upstream.

C = critical condition.

This curve gives a similar solution to Pearce's conclusion. However, the total pressure ratio, P_{t4}/P_{t0} (Ref. 8), is based on the time averaged value. This time averaged pressure ratio is not adequate as a parameter of the stability criterion, because during the buzz, or even in a quasi-steady flow condition, the flow in the diffuser cannot reach

an equilibrium condition. Therefore, the time averaged plenum total pressure, P_{t_4}, which is measured downstream of the unsteady shock wave during the buzz, cannot be a representative pressure. This is why the buzz occurs even at the zero or negative slope of the characteristic curve, D, based on the time averaged total pressure. It should be noted that Pearce and Trimpi obtained the characteristic curve based on the instantaneous pressure, and the results indicate that the buzz occurs only when the slope, D, reaches a certain positive value. When the frequency of the flow instability was analyzed, they treated the diffuser and the combustion chamber as a Helmholtz resonator. The propagated waves with spherical instead of flat surfaces are dumped out into the combustion with a hypothetical sudden expansion geometry. Therefore, these physical differences deduce an incorrect answer.

Trimpi (Refs. 3 and 4) investigated this problem theoretically and experimentally. His theory on the flow instability is based on the unsteady quasi-one-dimensional gasdynamics. He simplified the equations by using several assumptions in an attempt to reduce a laborious step-by-step calculation. He calculated the local static pressure during the buzz and obtained a good agreement with his experimental data. The assumptions he used in this theory are:

1. Gradual variations in the diffuser cross sectional area are accumulated and treated as discontinuous area changes (see Fig. 10).

2. Flow is isentropic in the duct. Entropy increases only when the flow passes across a normal shock or an oblique shock.

3. All the minor transmitted and reflected waves may be accumulated with the major transmitted and reflected waves; consequently, the group of waves is treated as one transmitted and one reflected wave.

4. The exit nozzle is operated at $M_{exit} = 1$.

5. Instead of the step-by-step procedure of constructing the characteristic lines with local slopes dependent on the sum or difference of the local flow velocity and sonic speed, the value of these speeds at the ends of the duct is used to obtain an average slope.

Trimpi also used experimental data as an initial condition of his calculation. Although his calculation results are in good agreement with his test results, there are a few points which require serious consideration.

Firstly, he has neglected the shock location during his calculation. This may be because the axial movement of the shock (velocity and location) is small in comparison with the chamber length, and because of a complexity in calculation. However, a reflected wave would have different properties (velocity, pressure, etc.) depending on the shock velocity and its moving direction. Secondly, an over simplification of the diffuser geometry gives an incorrect solution, especially the local pressure history of the subsonic diffuser section. Thirdly, a neglect of the local flow and acoustic velocity variation is somewhat dubious. When the change in local pressure with respect to time is large (for example, when the first expansion wave comes into the diffuser), this assumption is not valid. As a result, this theory by Trimpi is not suitable for explaining the buzz mechanism or the shock wave movement.

From Trimpi's theoretical and experimental investigations, he concluded that:

1. The flow instability is dependent on the instantaneous values of the mass flow and total pressure ratio, (P_{t4}/P_{to}), of the supersonic diffuser and immediate neighbouring subsonic diffuser.

2. The swallowed vortex sheet at the diffuser inlet is not an only criterion for the buzz initiation.

3. The buzz is caused by the wave pattern which consists of a downstream expansion reflected at the exit as an upstream expansion, and a downstream compression reflected as an upstream compression, plus several compression-expansion couples following the basic cycle. A pressure history based on this theory is reproduced in Fig. 11.

During his testing, Trimpi found that a flow separation on the center body can also be a cause of the buzz as Dailey later confirmed.

According to Ref. 10, Trimpi's theory does not require the blocking or choking of the air flow at the inlet lip of the diffuser to initiate the buzz, and therefore his theory is contradictory to Dailey's conclusion. However, Trimpi stated in his report (Ref. 3) that the buzz cycle started when a vortex sheet generated at the triple point of the shock system, (see Fig. 6), is swallowed in the diffuser. Furthermore, during his later experiment (Ref. 4), he found that the buzz could start when a strong flow separation occured on the center body in front of the inlet lip. In this case, the vortex sheet was far outside of the stagnatic streamline. Since a cons ble reduction of e ffe ive area at the inlet lip i ir rtant factor to initiate the buzz and that the area reduction is achieved by the flow separation or a thick boundary layer at the

inlet lip, one can say that their theories (Ferri and Nucci, Dailey, and Trimpi) are deduced from the same physical phenomenon. Trimpi's observation confirmed theories by Ferri and Nucci and also by Dailey even though there existed some arguments regarding the exact interpretation of the physical phenomenon (for example, whether or not the vortex sheet is the only cause of the buzz, or the complete mass flow cut-off can occur during the buzz, etc.)

Recently, researchers seem to have lost their interest in the investigation of the buzz mechanism possibly due to a complexity of the problem contributed by a significant effect of the flow viscosity, compressibility and unsteadiness. The viscous effect and the unsteady flow characteristics make it impossible to solve this problem with the existing gasdynamic theories. Nowadays, researchers are mainly interested in investigations to avoid the buzz phenomenon during the engine operation. However, it is the writer's opinion that the basic mechanism of the buzz phenomenon must first be understood before effective devices can be designed to eliminate it. The recent supersonic inlets practically used, have several devices to avoid the subcritical condition as shown in Fig. 12.

When the compressor inlet pressure increases, the bypass door is opened to bleed the air so that the shock is

kept just downstream of the diffuser throat (the optimum shock location), where the pressure ratio, P_{t4}/P_{t0}, is the maximum as seen in Fig. 3. On the other hand, if the compressor inlet pressure decreases, the bleed air is cut off and the inlet "barn door" opened to allow more mass flow in order to keep the maximum pressure ratio. To keep the optimum diffuser performance under various operating conditions with the above stated diffuser configuration, the following problems have to be solved:

1. Diffuser design to keep the shock wave at the optimum position (Refs. 15 to 17).

2. To keep the shock at the optimum position under various operating conditions, i.e. the take-off condition, the ground and flight idle conditions, the dive condition, the cruise condition, etc., an investigation to control the bypass door is necessary (Refs. 18 to 20).

3. To investigate the effective control, it is essential to know the shock wave dynamics. If any disturbance is propagated either from the upstream or the downstream to the shock, the shock is moved. Depending on the magnitude of the disturbance, the shock may over shoot and then move back. The shock may oscillate and finally rest at a new shock position. There have been many theoretical and/or experimental investigations

(for example, Refs. 21 to 26).

Unfortunately, no recent reference concerning the mechanism of the buzz and the organ pipe oscillation peculiar to the supersonic intake diffusers can be found. It is believed that unless a better understanding of this complex unsteady buzz phenomenon can be achieved, it will be rather difficult to attain optimum design of the supersonic intake diffuser.

2.2 HIGH FREQUENCY OSCILLATION

Stoolman (Ref. 11) and Mirels (Ref. 12) investigated the flow instability based on the acoustic impedence of the intake diffuser. Although the latter extended his theory to take into consideration the heat addition, both are generally based on the same approach. Stoolman's model is an open nose diffuser without a center body. He theoretically investigated a possibility of self-excitation of the acoustic wave and concluded that a criterion of the flow stability could be expressed in the following formula:

$$\left|\left\{\frac{1-\frac{\gamma-1}{2}M_5}{1+\frac{\gamma-1}{2}M_5}\right\}\left\{\frac{1+\zeta_4}{1-\zeta_4}\right\}\right| \begin{cases} > 1 & \text{unstable} \\ = 1 & \text{neutral} \\ < 1 & \text{stable} \end{cases}$$

where M = flow Mach number

$\zeta = (\bar{a}/\gamma\bar{p})(p'/u')$ = acoustic impedence

p = pressure

u = velocity

a = acoustic velocity

superscript, ' = perturbed value

superscript, - = average value

subscript, 4 = plenum chamber (Fig. 1)

subscript, 5 = exit nozzle (Fig. 1)

The first bracket of the above formula is the amplitude ratio of the reflected wave to the impinging wave at the

exit nozzle. The second bracket contains the amplitude ratio of the reflected wave to the impinging wave at the inlet of the plenum chamber. Mirels (Ref. 12) reached a similar conclusion. According to Stoolman's testing, the frequency of the self-excited oscillation is approximately equal to that of the first mode of the duct natural frequency, i.e. the diffuser length $\approx$ a quarter of the wave length.

Chang and Hsu (Ref. 9) analyzed the flow instability theoretically, based on the unsteady quasi-one-dimensional gas dynamics. They calculated a possible condition of the unstable flow analytically, using Stoolman's stability criterion. They are the first investigators who mathematically included the flow dynamics in the external compression region, i.e. the region between the expelled shock and the inlet lip. Their theoretical model is the same as that of Stoolman's, an open nose diffuser without a center body. Eventually, they showed that the flow instability would not occur without a viscous dissipation.

Although their theory is practical because it includes the flow dynamics in the external compression region and a viscous effect besides the compressibility and the unsteadiness, its accuracy is questionable. Among several assumptions they used, the assumption that $\frac{\partial}{\partial x}(A'/\bar{A}) \approx 0$ is doubtful (where $\bar{A}$ is an average flow cross sectional area

in the external compression region and a function of location x; A' is an area perturbation at the same location of $\bar{A}$; A' is a function of time, t, and location x; the location x is taken parallel to the intake axis and its origin is located at the inlet lip). If this assumption were true, then $(A'/\bar{A})_{x=0} \approx (A'/\bar{A})_{x\neq 0}$. Since the flow cross sectional area is almost constant at the inlet lip, (it should be noted that a flow area reduction at the inlet lip during the buzz is not considered in this theory), then A' = 0 at x = 0. Therefore, $(A'/\bar{A})_{x=0} = 0$ and $(A'/\bar{A})_{x\neq 0} \approx 0$. This means that the perturbed flow area in the external compression region is neither a function of location nor time. In other words, $A' \approx 0$. This means that the steady state condition is used in their theory as far as the flow area in the external compression region is concerned. However, the steady state condition cannot be attained during the unstable flow condition.

Thus, the two theories deduce different conclusions although they use the same basic theory and model. These differences in conclusions are due to:

1. Stoolman and Mirels considered the wave propagation only in the combustion chamber. Chang and Hsu took the external compression region into consideration as well as the internal compression region in their theory.

2. Stoolman and Mirels neglected the viscous effect.

3. Chang and Hsu used an incorrect assumption for the flow area in the external compression region.

4. Assumptions in formulae for the solutions of the basic equation are different. For example, the non-dimensionalized perturbed pressure:

$$\frac{p'}{\bar{p}} = F e^{i\left[\frac{k}{a}\left(\frac{x}{1+M}\right) - at\right]} + G e^{-i\left[\frac{k}{a}\left(\frac{x}{1+M}\right) + at\right]} \quad \text{(Stoolman-Mirels Theory)}$$

$$\frac{p'}{\bar{p}} = Q e^{i\omega t} \quad \text{(Chang-Hsu Theory)}$$

where, F,G,k = complex constants

a = acoustic speed

x = location

M = flow Mach number

t = time

$\omega = 2\pi f$

f = frequency

Q = real function of x

p' = perturbed pressure

$\bar{p}$ = average static pressure

An effect of a flow Mach number on the natural frequency and the damping characteristics of the flow fluctuation in a constant area duct was investigated by Whitehead (Ref. 13).

His conclusion indicates that the natural frequency reduces by increasing the duct flow Mach number, i.e. the natural frequency decreases when the mass flow increases, as shown below.

$$f = \left(\frac{n}{2} - \frac{1}{4}\right) \frac{a}{l} (1 - M^2)$$

where, n = 1, 2, 3, ...= mode

f = duct natural frequency

a = acoustic speed

l = duct length

M = flow Mach number in the duct

In case of zero mass flow, $f = \left(\frac{n}{2} - \frac{1}{4}\right) \frac{a}{l}$. This is the typical natural frequency of the organ pipe oscillation. A logarithmic ratio of the amplitude of the oscillation defined below shows that the damping is directly affected by the flow Mach number in the duct.

$$\delta = \ln \frac{e^{\alpha t}}{e^{\alpha(t+\tau)}} = \frac{2}{(2n-1)} \ln \frac{(1+M)}{(1-M)} \frac{(1+KM)}{(1-KM)}$$

where, δ = logarithmic ratio of two successive amplitudes

$e^{\alpha t}$ = amplitude of vibration at t = t

τ = period of oscillation

n = mode of oscillation

M = duct flow Mach number

K = f(M & M_e) (K = 0.2 at M_e = 1, γ = 1.4)

M_e = flow Mach number at exit nozzle

From the above formula, it is obvious that the flow becomes unstable more at low or zero mass flow conditions (where M is close or equal to zero) than at a high mass flow condition (where $0 < M < 1$).

Qualitatively, this theory is applicable to the present high frequency oscillation problem. However, since it does not include the effect of the shock movement in front of the duct, this theory does not provide a unique solution for the problem. In addition, this theory has neglected the viscous effect and the compressibility of the flow.

Trimpi and Dailey observed the high frequency oscillation during their experiments. According to Trimpi, a high frequency of 900 cps superimposed in the buzz cycle of 160 cps. When the exit valve is closed slightly, the high frequency changes into 1400 cps and the high frequency oscillation becomes even more dominant. Dailey reported the high frequency oscillation in more detail. He observed the high frequency oscillation during each buzz cycle and at zero mass flow condition. The frequency at the former condition was higher than that at the latter condition, as shown below. This tendency, however, is in contradiction to Trimpi's observation.

Diffuser Length (ft)	Mass Flow	Experimental Freq. (cps)	Nearest Organ Pipe Freq. (cps)	Mode	Re Number Based on Cowl Dia.
7.83	0	607	604	8	$.72 \times 10^6$
7.83	>0	690	685	9	$.72 \times 10^6$
1.89	0	470	460	2	$.74 \times 10^6$
1.89	>0	940	767	3	$.74 \times 10^6$
1.59 (Ref. 4)	>0	900	870	5	2.9×10^6 to 3.6×10^6
1.59 (Ref. 4)	>0	1400	1450	8	2.9×10^6 to 3.6×10^6

Table 1 High Frequency Oscillation

(Data obtained from Ref. 1)

The experimental data strongly indicate that the high frequency oscillation is of the typical organ pipe oscillation. However, no existing theory can tell which mode of the oscillation appears in which condition, because no serious attempt has been made to carry out a complete analysis of the shock in front of the inlet lip. In fact, if the high frequency oscillation occurred without the shock (the theory in Ref. 1 holds for the case), an open nose subsonic diffuser would have to suffer from this problem. However, this has never actually occured. The shock

oscillation in the supersonic diffuser results from the interaction of two groups of waves, one of which is generated and propagated between the inlet lip and the nozzle exit of the diffuser, and the other between the subcritical shock and the inlet lip.

3. THEORETICAL ANALYSIS OF FLOW OSCILLATION

3.1 LOW FREQUENCY OSCILLATION

As discussed in the last section, much work has been done on the low frequency oscillation, the buzz, by many researchers. At the present stage, at least the following phenomena are known concerning the buzz:

1. The buzz occurs at the subcritical condition.

2. A reduction of the inlet mass flow due to the flow separation at the inlet lip associates with the forward movement of the shock.

3. The buzz initiation mechanism is still unknown. However, it has been proved experimentally that the reflected perturbed acoustic waves in the diffuser are not responsible for the buzz initiation. The buzz starts in an abrupt and random manner.

4. Pressure history in the diffuser is well explained by using the one-dimensional characteristic method proposed by Trimpi. Although it was necessary for him to use experimental data as a boundary condition for his theoretical calculations, his solution is in good agreement with the experimental results. However, his "simplified" one-dimensional non-stationary wave theory

is still too tedious to be of much significant practical value.

Considering these facts, it can be said that more work is necessary on the following:

1. Discovering the real starting mechanism of the buzz.

2. Developing a more simplified theory for the flow characteristics (pressure, mass flow, etc.) during the buzz.

3.1.1 Interaction between Shock Wave and Isentropic Perturbations

As discussed in Section 1, there is a point of critical stability. For example, a spike diffuser has the point B in Fig. 3, and point A in Fig. 3 for an open nose diffuser. By adjusting the exit nozzle area, i.e. reducing the area, one can move the shock from its supercritical position to the point of the critical stability. If the diffuser is operated at this condition, the flow in the diffuser must still be stable. According to the test results, (Refs. 1, 3, etc.), the buzz can occur at this condition without any further exit nozzle area reduction. Therefore, some disturbance must result in a forward movement of the shock from its position of the critical stability. In this section, the effect of interaction between the disturbance and the shock

is considered for an open nose intake diffuser as shown in Fig. 4. It should be noted that this analysis can also be applicable to a spike diffuser, since the triple point of the shocks is far outside of the inlet cowl at this condition (see Fig. 13). However, in the case of the spike diffuser, the Station "0" corresponds to a point just upstream of the normal shock. Since the flow is steady and one-dimensional, the basic equations without the disturbances are:

$$\rho_0 u_0 = \rho_1 u_1 \qquad \text{(continuity)} \qquad (3.1\text{-}1)$$

$$\rho_0 u_0^2 + p_0 = \rho_1 u_1^2 + p_1 \qquad \text{(momentum)} \qquad (3.1\text{-}2)$$

$$C_p J g T_0 + \frac{u_0^2}{2} = C_p J g T_1 + \frac{u_1^2}{2} \qquad \text{(energy)} \qquad (3.1\text{-}3)$$

$$p_0 = \rho_0 R T_0 \quad , \quad p_1 = \rho_1 R T_1 \qquad \text{(state)} \qquad (3.1\text{-}4)$$

where, subscript 0=upstream of the normal shock (see Fig. 4)

subscript 1=downstream of the normal shock,

(see Fig. 4).

The flow is assumed to be non-viscous, thermodynamically perfect and isentropic except for the flow process across the shock. The coordinate is fixed to the normal shock.

Suppose that disturbances, i.e. isentropic waves, come from the upstream denoted by "ı" and the downstream denoted by "ıı", then the basic equations are:

$$(\rho_0+\rho_0')(u_0+u_0'-\xi) = (\rho_1+\rho_1'+\rho_1'')(u_1+u_1'+u_1''-\xi)$$

(continuity) (3.1-5)

$$(\rho_0+\rho_0')(u_0+u_0'-\xi)^2+(p_0+p_0') = (\rho_1+\rho_1'+\rho_1'')(u_1+u_1'+u_1''-\xi)^2+(p_1+p_1'+p_1'')$$

(momentum) (3.1-6)

$$C_p J g(T_0+T_0')+\frac{(u_0+u_0'-\xi)^2}{2} = C_p J g(T_1+T_1'+T_1'')+\frac{(u_1+u_1'+u_1''-\xi)^2}{2}$$

(energy) (3.1-7)

$$(p_0+p_0') = (\rho_0+\rho_0')R(T_0+T_0'), \quad (p_1+p_1'+p_1'') = (\rho_1+\rho_1'+\rho_1'')R(T_1+T_1'+T_1'')$$

(state) (3.1-8)

where, ξ = perturbed velocity of the shock.

Neglecting the second and the higher order of the perturbed terms, one can simplify the above equations:

$$\rho_0 u_0 + \rho_0(u_0'-\xi)+\rho_0' u_0 = \rho_1 u_1 + \rho_1(u_1'+u_1''-\xi)+(\rho_1+\rho_1'')u_1$$

$$\rho_0 u_0^2+2\rho_0 u_0(u_0'-\xi)+\rho_0' u_0^2+p_0+p_0' = \rho_1 u_1^2+2\rho_1 u_1(u_1'+u_1''-\xi)+(\rho_1'+\rho_1'')u_1^2 + p_1+p_1'+p_1''$$

$$C_p J g(T_0+T_0')+\frac{u_0^2}{2}+u_0(u_0'-\xi) = C_p J g(T_1+T_1'+T_1'')+\frac{u_1^2}{2}+u_1(u_1'+u_1''-\xi)$$

$$p_0+p_0' = \rho_0 R T_0 + \rho_0 R T_0' + \rho_0' R T_0, \quad p_1+p_1'+p_1'' = (\rho_1'+\rho_1'')RT_1+\rho_1 R(T_1'+T_1'')$$

Combining the above formulae with Eqns.(3.1-1) to (3.1-4) the following equations can be obtained:

$$\rho_0(u_0'-\xi)+\rho_0'u_0=\rho_1(u_1'+u_1''-\xi)+(\rho_1'+\rho_1'')u_1$$

(continuity) (3.1-9)

$$p_0'+2\rho_0u_0(u_0'-\xi)+\rho_0'u_0^2=(p_1'+p_1'')+2\rho_1u_1(u_1'+u_1''-\xi)+(\rho_1'+\rho_1'')u_1^2$$

(momentum) (3.1-10)

$$C_pJgT_0'+u_0(u_0'-\xi)=C_pJg(T_1'+T_1'')+u_1(u_1'+u_1''-\xi)$$

(energy) (3.1-11)

$$\frac{p_0'}{p_0}=\frac{T_0'}{T_0}+\frac{\rho_0'}{\rho_0}\quad,\qquad \frac{(p_1'+p_1'')}{p_1}=\frac{(\rho_1'+\rho_1'')}{\rho_1}+\frac{(T_1'+T_1'')}{T_1}$$

(state) (3.1-12)

In the same manner, the entropy perturbation can be expressed as:

$$\left.\begin{aligned}\frac{s_0'}{C_p}&=\frac{T_0'}{T_0}-\frac{(\gamma-1)}{\gamma}\left(\frac{p_0'}{p_0}\right)\\ \frac{s_1'}{C_p}&=\frac{T_1'}{T_1}-\frac{(\gamma-1)}{\gamma}\left(\frac{p_1'}{p_1}\right)\\ \frac{s_1''}{C_p}&=\frac{T_1''}{T_1}-\frac{(\gamma-1)}{\gamma}\left(\frac{p_1''}{p_1}\right)\end{aligned}\right\} \qquad (3.1\text{-}13)$$

However, since the isentropic perturbations are considered,

$$\frac{s_0'}{C_p}=\frac{s_1''}{C_p}=0$$

Therefore, Eqn.(3.1-13) becomes:

$$\left.\begin{aligned} \frac{T_0'}{T_0} &= \frac{(\gamma-1)}{\gamma}\left(\frac{P_0'}{P_0}\right) \\ \frac{S_1'}{C_p} &= \frac{T_1'}{T_1} - \frac{(\gamma-1)}{\gamma}\left(\frac{P_1'}{P_1}\right) \\ \frac{T_1''}{T_1} &= \frac{(\gamma-1)}{\gamma}\left(\frac{P_1''}{P_1}\right) \end{aligned}\right\} \qquad (3.1\text{-}14)$$

A relationship between the perturbed pressure and the perturbed velocity can be obtained by solving the equations concerning their time-and-space-dependent characteristics. Considering the perturbation characteristics, the coordinate used below is moved with the main flow of which velocity is U_0. Then the basic equations for the perturbation are:

$$\frac{\partial(\rho_0+\rho_0')}{\partial t} + (\rho_0+\rho_0')\frac{\partial u_0'}{\partial x} + u_0'\frac{\partial(\rho_0+\rho_0')}{\partial x} = 0 \quad \text{(continuity)} \qquad (3.1\text{-}15)$$

$$\frac{\partial u_0'}{\partial t} + u_0'\frac{\partial u_0'}{\partial x} = -\frac{1}{(\rho_0+\rho_0')}\frac{\partial(P_0+P_0')}{\partial x} \quad \text{(momentum)} \qquad (3.1\text{-}16)$$

Since

$$\frac{\partial(P_0+P_0')}{\partial x} = \frac{d(P_0+P_0')}{d(\rho_0+\rho_0')}\frac{\partial(\rho_0+\rho_0')}{\partial x} \approx a_0^2\frac{\partial(\rho_0+\rho_0')}{\partial x}$$

Eqn.(3.1-16) can be re-written as follows:

$$\frac{\partial u_0'}{\partial t} + u_0'\frac{\partial u_0'}{\partial x} = -\frac{a_0^2}{(\rho_0+\rho_0')}\frac{\partial(\rho_0+\rho_0')}{\partial x} \qquad (3.1\text{-}16')$$

Define the condensation, $\tilde{s}$, such that;

$$\tilde{s} = \frac{\rho_0'}{\rho_0} \qquad (3.1\text{-}17)$$

By using Eqn.(3.1-17), the continuity equation and the momentum equation become:

$$\rho_0 \frac{\partial \tilde{s}}{\partial t} + \rho_0 \left(\frac{\partial u_0'}{\partial x} + \tilde{s} \frac{\partial u_0'}{\partial x} \right) + \rho_0 u_0' \frac{\partial \tilde{s}}{\partial x} = 0 \qquad (3.1\text{-}18)$$

$$\frac{\partial u_0'}{\partial t} + u_0' \frac{\partial u_0'}{\partial x} + \frac{a_0^2}{1+\tilde{s}} \frac{\partial \tilde{s}}{\partial x} = 0 \qquad (3.1\text{-}19)$$

Since the flow is one-dimensional and the perturbation is so small, u_0', $\tilde{s}$, $\partial u_0'/\partial x$ & $\partial \tilde{s}/\partial x$ must also be small. As a first order approximation, the second and the higher order terms are assumed to be negligible. Then, the above formulae become:

$$\rho_0 \frac{\partial \tilde{s}}{\partial t} + \rho_0 \frac{\partial u_0'}{\partial x} = 0$$

or

$$\frac{\partial \tilde{s}}{\partial t} + \frac{\partial u_0'}{\partial x} = 0 \qquad (3.1\text{-}20)$$

and

$$\frac{\partial u_0'}{\partial t} + a_0^2 \frac{\partial \tilde{s}}{\partial x} = 0 \qquad (3.1\text{-}21)$$

From Eqns.(3.1-20) and (3.1-21), the following equations are obtained:

$$\frac{\partial^2 \tilde{s}}{\partial t^2} - a_0^2 \frac{\partial^2 \tilde{s}}{\partial x^2} = 0 \qquad (3.1\text{-}22)$$

$$\frac{\partial^2 u_0}{\partial t^2} - a_0^2 \frac{\partial^2 u_0}{\partial x^2} = 0 \qquad (3.1\text{-}23)$$

The above are the wave equations. Therefore, the general solution has the following form:

$$\tilde{s} = F(x - a_0 t) + G(x + a_0 t) \qquad (3.1\text{-}24)$$

where, F and G are arbitrary functions of $(x-a_0t)$ and $(x+a_0t)$, respectively.

Similarly,

$$u_0' = f(x-a_0t) + g(x+a_0t) \tag{3.1-25}$$

where, f and g are arbitrary functions of $(x-a_0t)$ and $(x+a_0t)$, respectively.

Substituting Eqns.(3.1-24) and (3.1-25) into Eqn.(3.1-20), relationships between f (and g) and F (and G) are expressed as follows:

$$\frac{\partial \tilde{s}}{\partial t} = -a_0 \frac{dF}{d(x-a_0t)} + a_0 \frac{dG}{d(x+a_0t)}$$

$$\frac{\partial u_0'}{\partial x} = \frac{df}{d(x-a_0t)} + \frac{dg}{d(x+a_0t)}$$

Therefore,

$$\frac{d(f-a_0F)}{d(x-a_0t)} + \frac{d(g+a_0G)}{d(x+a_0t)} = 0$$

Since the above relationships hold for arbitrary functions of F, G, f and g,

$$\left.\begin{aligned} f &= a_0 F \\ g &= -a_0 G \end{aligned}\right\} \tag{3.1-26}$$

is sufficient to satisfy Eqns.(3.1-20) and (3.1-21). When G = 0, then g = 0,

$$\tilde{s} = F(x-a_0t) = \frac{1}{a_0} f(x-a_0t) = \frac{u_0'}{a_0} \tag{3.1-27}$$

This indicates a wave which propagates downstream with a velocity of sound relative to the flow velocity. On the other hand, when $F = f = 0$,

$$\tilde{S} = G(x - a_0 t) = -\frac{1}{a_0} g(x + a_0 t) = -\frac{u_0'}{a_0} \qquad (3.1\text{-}28)$$

The wave expressed by the above formula propagates upstream with an acoustic velocity relative to the flow velocity.

Since the perturbation is isentropic,

$$\left(\frac{p_0 + p_0'}{p_0}\right) = \left(\frac{\rho_0 + \rho_0'}{\rho_0}\right)^{\gamma} = (1 + \tilde{S})^{\gamma} \approx 1 + \gamma \tilde{S}$$

Therefore,

$$\frac{p_0'}{p_0} \approx \gamma \tilde{S} \qquad (3.1\text{-}29)$$

Combining Eqn.(3.1-29) with Eqns.(3.1-27) and (3.1-28), one obtains:

$$\frac{p_0'}{p_0} = \pm \gamma \frac{u_0'}{u_0}$$

or

$$p_0' = \pm \frac{\gamma p_0}{a_0} u_0' = \pm a_0 \rho_0 u_0' \qquad (3.1\text{-}30)$$

where, +ve shows a wave propagating downstream, and
-ve shows a wave propagating upstream.

Eqn.(3.1-30) is the relationship between the perturbed pressure and the perturbed velocity. Thus, all the basic equations used to investigate the interaction between the disturbances and the shock have been deduced.

There are three possible cases of interactions:

Case 1 The disturbances collide head on with the shock.

Case 2 The shock catches up with the disturbances.

Case 3 The disturbances catch up with the shock.

3.1.1a Perturbation Generated in the Upstream of the Shock

When the perturbation, i.e. the isentropic wave, is generated in the upstream of the shock, Case 1 and Case 2 of the above stated cases can exist. Both of these two cases are shown on a time-space diagram in Fig. 14. The perturbed shock velocity, "ξ", has either a positive sign if the isentropic wave is a rarefaction wave, or a negative sign if the wave is a compression wave.

Since the disturbance is propagated from the upstream of the shock, all the quantities of the disturbance generated from the downstream of the shock denoted by the superscript ", are zero. Therefore, Eqns.(3.1-9) to (3.1-12) are re-written as follows:

$$\rho_0(u_0-\xi)+\rho_0' u_0 = \rho_1(u_1'-\xi)+\rho_1' u_1 \quad \text{(continuity)} \quad (3.1\text{-}31)$$

$$p_0' + 2\rho_0 u_0 (u_0' - \xi') + \rho_0' u_0^2 = p_1 + 2\rho_1 u_1 (u_1' - \xi') + \rho_1' u_1^2$$

(momentum) (3.1-32)

$$C_p J_g T_0' + u_0 (u_0' - \xi') = C_p J_g T_1' + u_1 (u_1' - \xi') \quad \text{(energy)} \qquad (3.1\text{-}33)$$

$$\frac{p_0'}{p_0} = \frac{T_0'}{T_0} + \frac{\rho_0'}{\rho_0}, \qquad \frac{p_1'}{p_1} = \frac{T_1'}{T_1} + \frac{\rho_1'}{\rho_1} \qquad \text{(state)} \qquad (3.1\text{-}34)$$

From Eqn.(3.1-30), one obtains:

$$p_0' = \pm a_0 \rho_0 u_0' \qquad (3.1\text{-}35)$$

$$p_1' = a_1 \rho_1 u_1' \qquad (3.1\text{-}36)$$

where, +ve sign indicates a wave propagating downstream, and
-ve sign indicates a wave propagating upstream.

It should be noted that the right hand side of Eqn.(3.1-36) has a positive sign only, since the disturbance cannot be reflected to the upstream of the shock, i.e. the disturbance cannot have a -ve sign, because the upstream velocity is supersonic.

Substituting Eqns.(3.1-14), (3.1-34), (3.1-35) and (3.1-36) into Eqn.(3.1-32), one obtains:

$$\frac{\rho_0}{\rho_1}(1 \pm M_0)^2 \frac{p_0'}{\rho_0} = (1 + M_1)^2 \frac{p_1'}{p_1} - (\gamma - 1) M_1^2 s_1' T_1 \qquad (3.1\text{-}37)$$

The same substitution into Eqn.(3.1-33) results in:

$$\left\{(1\pm M_0)\left(1\pm\frac{\rho_0}{\rho_1}M_0\right)\right\}=\left\{(1+M_1)\left(1+\frac{\rho_1}{\rho_0}M_1\right)\right\}\frac{p_1'}{\rho_1}+\left\{1-(\gamma-1)M_1^2\frac{\rho_1}{\rho_0}\right\}s_1'T_1 \qquad (3.1\text{-}38)$$

Eliminating the entropy perturbation, s_1', from Eqns.(3.1-37) and (3.1-38), the downstream pressure perturbation, p_1', can be expressed as a function of the upstream pressure perturbation, p_0', i.e.:

$$\frac{p_1'}{p_0'}=\frac{\left(\frac{\rho_1}{\rho_0}\right)(1\pm M_0)\left[(1\pm M_0)\left\{1-(\gamma-1)M_1^2\frac{\rho_1}{\rho_0}\right\}\frac{\rho_0}{\rho_1}+(\gamma-1)M_1^2\left(1\pm\frac{\rho_0}{\rho_1}M_0\right)\right]}{(1\pm M_1)\left[(1+M_1)\left\{1-(\gamma-1)M_1^2\frac{\rho_1}{\rho_0}\right\}+\left(1+\frac{\rho_1}{\rho_0}M_1\right)(\gamma-1)M_1^2\right]}$$

or:

$$p_1'=\left\{{}_pT_p\right\}p_0' \qquad (3.1\text{-}39)$$

where, $${}_pT_p=\frac{\left(\frac{\rho_1}{\rho_0}\right)(1\pm M_0)\left[(1\pm M_0)\left\{1-(\gamma-1)M_1^2\frac{\rho_1}{\rho_0}\right\}\frac{\rho_0}{\rho_1}+(\gamma-1)M_1^2\left(1\pm\frac{\rho_0}{\rho_1}M_0\right)\right]}{(1\pm M_1)\left[(1+M_1)\left\{1-(\gamma-1)M_1^2\frac{\rho_1}{\rho_0}\right\}+\left(1+\frac{\rho_1}{\rho_0}M_1\right)(\gamma-1)M_1^2\right]}$$

which is called the transmission coefficient of an isentropic pressure pulse through a normal shock in Ref. 14.

In the above equation, a +ve sign holds for Case 1 where the disturbance collides head on with the shock, and a -ve sign holds for Case 2 where the shock catches up with the disturbance.

By eliminating the downstream perturbation term, $\frac{p_1'}{\rho_1'}$, in Eqns.(3.1-37) and (3.1-38), and considering that $\frac{s'}{c_p} \approx \frac{T_1'}{T_1}$ (see Eqn.(3.1-14)), one can obtain the downstream disturbance in terms of the temperature which is expressed as a function of the upstream pressure perturbation.

$$T_1' \approx \frac{s_1' T_1}{c_p} = \frac{p_0'}{\rho_0 c_p} \left\{ {}_p T_T \right\} \tag{3.1-40}$$

where, $$\left\{ {}_p T_T \right\} = \frac{(1 \pm M_0)\left\{(1+M_1)(1 \pm \frac{\rho_0}{\rho_1} M_0) - (1 \pm M_0)(1+\frac{\rho_1}{\rho_0} M_1)\frac{\rho_0}{\rho_1}\right\}}{(1+M_1) - (\gamma-1) M_1^2 (\frac{\rho_1}{\rho_0} - 1)}$$

Similarly, the perturbed shock velocity, ξ, can be expressed as a function of u_0', by substituting Eqns.(3.1-39) and (3.1-40) into Eqn.(3.1-31).

$$\xi = \left\{ {}_p T_\xi \right\} u_0' \tag{3.1-41}$$

where, $${}_p T_\xi = \frac{1}{(1-\frac{\rho_1}{\rho_0})} \left\{ (1 \pm M_0) \mp (\frac{a_0}{a_1})(1+\gamma M_1)\left\{ {}_p T_p \right\} + \frac{\rho_1}{\rho_0}\frac{a_0}{a_1} M_1 \left\{ {}_p T_T \right\} \right\}$$

The transmission coefficients, ${}_p T_p$, ${}_p T_T$ and ${}_p T_\xi$, are calculated and shown in Figs. 15 and 16 ($\gamma = 1.4$ is assumed). It is obvious from Figs. 15 and 16 that the pressure and temperature perturbation is amplified by the interaction at high free stream Mach number. The interaction between the shock and the perturbation colliding head on always amplifies the pressure perturbation. Because of the interaction, the perturbed shock velocity, ξ, is about the same

order of the upstream perturbation velocity, u_0', except for the head on collision (see Fig. 15) at low supersonic upstream Mach number. Therefore, it can be said that the shock is moved by the upstream perturbation and that the downstream perturbation is amplified by the perturbation-shock interaction.

3.1.1b Perturbation Generated in the Downstream of the Shock

When the perturbation is generated in the downstream of the shock, Case 3 occurs. Since there are no upstream disturbances, all the properties denoted by a combination of a superscript,', and a subscript,0, are zero. Then Eqns.(3.1-9) to (3.1-12) become:

$$-\rho_0 \xi = \rho_1 (u_1' + u_1'' - \xi) + (\rho_1' + \rho_1'') u_1 \quad \text{(continuity)} \quad (3.1\text{-}42)$$

$$-2\rho_0 u_0 \xi = (p_1' + p_1'') + 2\rho_1 u_1 (u_1' + u_1'' - \xi) + (\rho_1' + \rho_1'') u_1^2 \quad \text{(momentum)} \quad (3.1\text{-}43)$$

$$-u_0 \xi = c_p J g (T_1' + T_1'') + u_1 (u_1' + u_1'' - \xi) \quad \text{(energy)} \quad (3.1\text{-}44)$$

$$\frac{p_1' + p_1''}{p_1} = \frac{T_1' + T_1''}{T_1} + \frac{\rho_1' + \rho_1''}{\rho_1} \quad \text{(state)} \quad (3.1\text{-}45)$$

It is understood that the disturbances must be propagated upstream to meet the shock and then reflected downstream . Eqn.(3.1-30) may be expressed as:

$$p_1'' = -a_1 \rho_1 u_1'' \tag{3.1-46}$$

$$p_1' = a_1 \rho_1 u_1' \tag{3.1-47}$$

Similar to the previous case (Section 3.1.1a), the momentum and energy equations combining with the equation of state (Eqn.(3.1-45)) and the isentropic relationship (the second and third equations of Eqn.(3.1-14)) take the following form:

$$(1+M_1)^2 p_1' + (1-M_1)^2 p_1'' - (\gamma-1)\rho_1 M_1^2 S_1' T_1 = 0 \tag{3.1-48}$$

$$\left\{(1+M_1)\left(1+\frac{\rho_1}{\rho_0}M_1\right)\right\}\frac{p_1'}{\rho_1} + \left\{(1-M_1)\left(1-M_1\frac{\rho_1}{\rho_0}\right)\right\}\frac{p_1''}{\rho_1} + \left\{1-\frac{\rho_1}{\rho_0}(\gamma-1)M_1^2\right\} S_1' T_1 = 0 \tag{3.1-49}$$

Eliminating the entropy perturbation, S', from the above equations, one obtains:

$$p_1' = \{{}_pR_p\}\, p_1'' \tag{3.1-50}$$

where,

$$\{{}_pR_p\} = -\frac{(1-M_1)\left\{(1-M_1)+(\gamma-1)\left(1-\frac{\rho_1}{\rho_0}\right)M_1^2\right\}}{(1+M_1)\left\{(1+M_1)+(\gamma-1)\left(1-\frac{\rho_1}{\rho_0}\right)M_1^2\right\}}$$

$\{{}_pR_p\}$ is called the coefficient of reflection of an isentropic pressure pulse reflected at the shock. An elimination of p_1' from Eqns.(3.1-48) and (3.1-49) gives:

$$T_1' = \{{}_pR_T\}\frac{p_1''}{C_p \rho_1} \tag{3.1-51}$$

where, $${}_pR_T = \frac{2M_1(1-M_1)(1-\frac{\rho_1}{\rho_0})}{(1+M_1)+(\gamma-1)M_1^2(1-\frac{\rho_1}{\rho_0})}$$

From Eqn.(3.1-42), the perturbed shock velocity, ξ, can be obtained as a function of the impinging perturbed velocity, u_1'', with the aid of Eqns.(3.1-50) and (3.1-51). Then

$$\xi = \left\{ {}_pR_\xi \right\} u_1'' \qquad (3.1\text{-}52)$$

where, $${}_pR_\xi = \frac{\rho_1}{(\rho_1-\rho_0)}\left\{(1-M_1)-(1+\gamma M_1)\left\{{}_pR_p\right\}+(\gamma-1)M_1\left\{{}_pR_T\right\}\right\}$$

The time-space diagram for this case and the coefficients of reflections, ${}_pR_p$, ${}_pR_T$ and ${}_pR_\xi$, are shown in Figs. 17 and 18 respectively. Calculation results indicate that the pressure perturbation is weakened by the interaction. This means that the reflected wave will not be amplified and the oscillation is not self-sustaining. However, the perturbed shock velocity, ξ, has the same order as the impinging perturbed velocity, u_1'', which means that the shock can be pushed forward or pulled backward by the downstream perturbation.

3.1.2 Consideration on Initiation of Buzz

According to the previous experimental investigations (for example, Refs. 1, 2, 3, 4, etc.) it was found that:

1. The buzz occurs abruptly and its frequency is quite random.

2. The iteratively reflected waves in the diffuser do not play an important role in initiating the buzz.

3. Whenever the buzz starts, the effective flow area at the diffuser inlet is small, due possibly to the flow separation.

Therefore, something which triggers the buzz must exist either upstream of,or at the diffuser inlet lip. One possibility is the small perturbations discussed in the previous section. As concluded, these isentropic perturbations can move the shock wave with about the same order of velocity as that of the perturbations. For example, if the perturbation is propagated from upstream of the shock as described in Section 3.1.1a, the perturbation is amplified across the shock and the shock wave is moved upstream, if the perturbation is a rarefaction wave; or downstream , if the perturbation is a compression wave. If the shock is moved upstream, the mass flow rate into the intake reduces. Then the static pressure rise between the shock and the inlet lip increases, resulting in either a thicker boundary layer or a flow separation on the center body of a spike diffuser. The effective flow area at the inlet lip reduces and consequently, a further mass flow reduction is required. This

signal is propagated as a compression wave to the shock. The shock is then forced to move further upstream, thus the [illegible] In this case, the separation induced by a vortex sheet generated at the shock triple point is not needed to start the buzz. This explanation agrees quite well with Dailey's and Trimpi's observation. If the buzz initiation is controlled by an upstream disturbance, it is not surprising that the buzz has a rather random frequency and occurs abruptly. If, on the other hand, the vortex sheet from the shock triple point is swallowed under the stable condition, i.e. the high subcritical condition, the flow area at the inlet lip reduces. If the flow separation is induced by this vortex sheet, the flow area reduction must be very severe. A compression wave is generated and propagated to the shock in order to adjust for the mass flow, and this is generally accomplished by moving the shock further upstream. This case is similar to that discussed in Section 3.1.1b. This may also be considered as one mechanism which starts the buzz, provided that the compression wave is strong enough for the shock to be moved beyond the position at which the stable condition starts to become unstable. This case was observed by Ferri and Nucci. However, if the compression wave is not strong enough, the shock can still be on the equilibrium condition, i.e. stable. When this happens, as pointed out by Dailey and Trimpi, the buzz does not occur. Even though this explanation does not conflict with the experimental results obtained by many

researchers, it is not absolutely sound for the following reasons:

1. If the upstream disturbance is a compression wave, the shock moves downstream and the disturbance is amplified across the shock. The above stated theory cannot explain how the shock and downstream disturbance behave afterwards, or whether or not this compression wave can initiate the buzz. It is especially essential to know the behavior of the downstream disturbance which is amplified when it passes through the shock at the inlet lip.

2. The buzz initiation in an open nose diffuser without a center body cannot be explained by the above mentioned theory.

Nevertheless, it is worth while to note that the upstream and downstream disturbances have a potential to start the buzz. This must be justified by an experimental investigation. At the same time, the more precise interaction between the shock and the isentropic waves must be understood.

3.1.3 Plenum Pressure During the Buzz Cycle

Trimpi attempted to calculate the local static pressure history in the diffuser during the buzz (Ref. 3). His theory is based on unsteady one-dimensional gasdynamics. As discussed in Section 2.1, Trimpi made several assumptions to simplify the equation in order to avoid the laborious work of the calculation. Although his solution is useful and provides good agreement with his particular test data, the calculation is still cumbersome.

Dailey (Ref. 1) presented the equation of the pressure in the diffuser only during the fill-up period. His theory is based on quasi-steady one-dimensional gasdynamics. The local pressure is only a function of time, not of location. In his theory, the flow Mach number is assumed to be unity at the diffuser throat and the exit nozzle. However, $M_{diff.\ throat}=1.0$ is not always correct during the fill-up period, because the normal shock is swallowed in the diffuser. Therefore, $M_{diff.\ throat}>1.0$ is possible, depending on the area ratio of the diffuser throat to the stagnation flow streamline in the infinite upstream and on the flight Mach number.

Since Trimpi's theory is difficult to apply and very time consuming and Dailey's theory is correct only at $M_{diff.throat}=1$, a new theoretical model is proposed based on the non-viscous and one-dimensional flow theory. Although an

open nose diffuser (see Fig. 4) is considered in this report, this theory is also applicable to a spike diffuser provided that an effect of the oblique shock in front of the diffuser inlet on the flow pattern is taken into consideration. This theory is not applicable when the flow has a strong separation in the diffuser.

From a definition of the Fliegner's number, F(M), one obtains:

$$F(M) = \frac{m\sqrt{JC_p T_t}}{A P_t \sqrt{g}} = \frac{\gamma}{\sqrt{\gamma-1}} M \left\{1 + \frac{\gamma-1}{2} M^2\right\}^{-\frac{(\gamma+1)}{2(\gamma-1)}} \qquad (3.1\text{-}53)$$

where, a subscript "t" denotes stagnation. Therefore, the mass flow rate is:

$$m = \frac{\sqrt{g} A P_t}{\sqrt{JC_p T_t}} \frac{\gamma}{\sqrt{\gamma-1}} M \left\{1 + \frac{\gamma-1}{2} M^2\right\}^{-\frac{(\gamma+1)}{2(\gamma-1)}} = \frac{g A P_t}{\sqrt{\gamma g R T_t}} \gamma M \left\{1 + \frac{\gamma-1}{2} M^2\right\}^{-\frac{(\gamma+1)}{2(\gamma-1)}}$$

$$\therefore m = \frac{g A P_t}{a_t} \gamma M \left\{1 + \frac{\gamma-1}{2} M^2\right\}^{-\frac{(\gamma+1)}{2(\gamma-1)}} \qquad (3.1\text{-}54)$$

where, a_t = acoustic velocity based on the stagnation property.

The mass flow rate into the diffuser is the mass flow rate at Station 3 in Fig. 4, hence:

$$m_3 = \frac{g A_3 P_{t_3}}{a_{t_3}} \gamma M_3 \left\{1 + \frac{\gamma-1}{2} M_3^2\right\}^{-\frac{(\gamma+1)}{2(\gamma-1)}} \qquad (3.1\text{-}55)$$

The out-flow is expressed as the mass flow rate at Station 5 in Fig. 4.

$$m_5 = \frac{g A_5 P_{t5}}{a_{t5}} \gamma M_5 \left\{1 + \frac{\gamma-1}{2} M_5^2\right\}^{-\frac{(\gamma+1)}{2(\gamma-1)}}$$

Since a choke condition is assumed at Station 5,

$$M_5 = 1$$

$$\therefore m_5 = \frac{g A_5 P_{t5}}{a_{t5}} \gamma \left\{\frac{\gamma+1}{2}\right\}^{-\frac{(\gamma+1)}{2(\gamma-1)}} \qquad (3.1\text{-}56)$$

The difference of the in-flow from the out-flow is accumulated in the plenum chamber, which causes the density increase in the plenum chamber.

$$\Delta m = m_3 - m_5 = V\frac{d\rho_4}{dt} = A_4 \ell \frac{d\rho_4}{dt} \qquad (3.1\text{-}57)$$

where, V = volume of the plenum chamber,

ℓ = equivalent axial length of the plenum chamber and is defined as $\ell = V/A_4$.

The flow is assumed to be isentropic at Station 4, thus:

$$\frac{P_4}{P_{t4}} = \left(\frac{\rho_4}{\rho_{t4}}\right)^{\gamma}$$

$$dP_4 = \frac{1}{\gamma}\left(\frac{\rho_{t4}}{P_{t4}}\right)\left(\frac{P_4}{P_{t4}}\right)^{\frac{1-\gamma}{\gamma}} d\rho_4 \qquad (3.1\text{-}58)$$

In the plenum chamber (between Stations 4 and 5 in Fig. 4), the flow Mach number is so low that $p_4 \approx P_{t4}$ can be assumed.

$$\therefore d\rho_4 \approx \frac{1}{\gamma}\frac{\rho_{t4}}{P_{t4}} dP_{t4}$$

Combining the equation of state with the above formula, the following relationship can be obtained:

$$d\rho_4 \approx g\frac{dP_{t4}}{\gamma g R T_{t4}} = g\frac{dP_{t4}}{a_{t4}^2} \tag{3.1-59}$$

$$\therefore \Delta m = m_3 - m_5 = V\frac{d\rho_4}{dt} \approx g\frac{A_4 \ell}{a_{t4}^2}\left(\frac{dP_{t4}}{dt}\right) \tag{3.1-60}$$

3.1.3a Discharge Period

During the discharge period, the normal shock is in front of the inlet lip (see Fig. 19). Also, no energy transfer is assumed in the flow between Station 0 and Station 5. Therefore,

$$\left.\begin{aligned}
&P_{t3} = P_{t1} = P_{t4} \\
&a_{t3} = \sqrt{\gamma g R T_{t3}} = \sqrt{\gamma g R T_{t0}} = a_{t0} \\
&\frac{A_0}{A_3} = \frac{A_1}{A_3} = \left\{\frac{M_3\left(1+\frac{\gamma-1}{2}M_3^2\right)}{M_1\left(1+\frac{\gamma-1}{2}M_1^2\right)}\right\}^{-\frac{(\gamma+1)}{2(\gamma-1)}} \\
&M_1^2 = \frac{M_0^2 + \frac{2}{(\gamma-1)}}{\frac{2\gamma}{(\gamma-1)}M_0^2 - 1} \\
&\frac{P_{t1}}{P_{t0}} = \left\{\frac{\frac{\gamma+1}{2}M_0^2}{1+\frac{\gamma-1}{2}M_0^2}\right\}^{\frac{\gamma}{\gamma-1}} \Big/ \left\{\frac{2\gamma}{\gamma+1}M_0^2 - \frac{\gamma-1}{\gamma+1}\right\}^{\frac{1}{\gamma-1}}
\end{aligned}\right\} \tag{3.1-61}$$

are obtained from the flow and shock relationships. If the upstream conditions are given, the flow condition at Station 3 can be calculated. From Eqns.(3.1-55) and (3.1-61),

$$m_3 = \frac{g A_3 P_{t_4}}{a_{t_0}} \gamma M_3 \left\{ 1 + \frac{\gamma-1}{2} M_3^2 \right\}^{-\frac{\gamma+1}{2(\gamma-1)}} \qquad (3.1\text{-}62)$$

At the exit, Station 5, $M_5=1$ is assumed. Therefore, from Eqn.(3.1-56),

$$m_5 = \frac{g A_5 P_{t_4}}{a_{t_0}} \gamma \left\{ \frac{\gamma+1}{2} \right\}^{-\frac{(\gamma+1)}{2(\gamma-1)}} \qquad (3.1\text{-}63)$$

where, $P_{t_4} = P_{t_5}$

$a_{t_5} = \sqrt{\gamma g R T_{t_5}} = \sqrt{\gamma g R T_{t_0}} = a_{t_0}$ were used.

Substituting them into Eqn.(3.1-60), one obtains:

$$m_3 - m_5 = g \frac{P_{t_4}}{a_{t_0}} \gamma \left[A_3 M_3 \left\{ 1 + \frac{\gamma-1}{2} M_3^2 \right\}^{-\frac{(\gamma+1)}{2(\gamma-1)}} - A_5 \left\{ \frac{\gamma+1}{2} \right\}^{-\frac{(\gamma+1)}{2(\gamma-1)}} \right] = g \frac{A_4 l}{a_{t_4}^2} \left(\frac{d P_{t_4}}{dt} \right)$$

Since,

$$a_{t_4}^2 = \gamma g R T_{t_4} = \gamma g R T_{t_0} = a_{t_0}^2$$

$$\frac{a_{t_0} \gamma}{l} \left[\frac{A_3}{A_4} M_3 \left\{ 1 + \frac{\gamma-1}{2} M_3^2 \right\}^{-\frac{(\gamma+1)}{2(\gamma-1)}} - \frac{A_5}{A_4} \left\{ \frac{\gamma+1}{2} \right\}^{-\frac{(\gamma+1)}{2(\gamma-1)}} \right] \frac{P_{t_4}}{P_{t_0}} = \frac{d\left(\frac{P_{t_4}}{P_{t_0}} \right)}{dt} \qquad (3.1\text{-}64)$$

In fact, M_3 is a function of time during the actual buzz cycle. Since this function is unknown and impossible to obtain theoretically, M_3 is assumed to be constant, as an

approximation. Then Eqn.(3.1-64) can be solved. This equation is re-written as follows:

$$K(C_1 - C_2)\frac{P_{t4}}{P_{t_0}} = \frac{d\left(\frac{P_{t4}}{P_{t_0}}\right)}{dt} \qquad (3.1\text{-}65)$$

where, $K = \frac{a_{t_0}\gamma}{\ell}$ =constant

$C_1 = \frac{A_3}{A_4} M_3 \left\{1 + \frac{\gamma-1}{2} M_3^2\right\}^{-\frac{(\gamma+1)}{2(\gamma-1)}}$ =non-dimensional constant

$C_2 = \frac{A_5}{A_4}\left\{\frac{\gamma+1}{2}\right\}^{-\frac{(\gamma+1)}{2(\gamma-1)}}$ =non-dimensional constant

A boundary condition of the integration of Eqn.(3.1-65) is $P_{t4} = P_{t4i}$ (the initial plenum total pressure) at t = 0. Therefore, Eqn.(3.1-65) can be integrated.

$$\int K dt = \frac{1}{(C_1 - C_2)} \int \frac{d(P_{t4}/P_{t_0})}{(P_{t4}/P_{t_0})} + C$$

$$Kt = \frac{1}{(C_1 - C_2)} \ln\left(\frac{P_{t4}}{P_{t_0}}\right) + C$$

where, $C = -\frac{1}{(C_1 - C_2)} \ln(P_{t4i}/P_{t_0})$

$$\therefore Kt = \frac{1}{(C_1 - C_2)} \ln\left(\frac{P_{t4}/P_{t_0}}{P_{t4i}/P_{t_0}}\right) \qquad (3.1\text{-}66)$$

or:

$$\frac{P_{t4}}{P_{t_0}} = \left(\frac{P_{t4i}}{P_{t_0}}\right) e^{(C_1 - C_2)Kt} \qquad (3.1\text{-}67)$$

where, $Kt = \frac{a_{t_0}\, \ell}{\gamma}\, t$ =non-dimensional constant

$C_1 = \frac{A_3}{A_4} M_3 \left\{ 1 + \frac{\gamma-1}{2} M_3^2 \right\}^{-\frac{(\gamma+1)}{2(\gamma-1)}}$ =non-dimensional constant

$C_2 = \frac{A_5}{A_4} \left\{ \frac{\gamma+1}{2} \right\}^{-\frac{(\gamma+1)}{2(\gamma-1)}}$ =non-dimensional constant

M_3 in C_1 and C_2 can be calculated with a normal shock relationship and basic equations for a compressible flow, knowing the flight Mach number, M_0 and the area ratio, A_0/A_3. Calculation results are presented in Fig. 20. During the start of the actual buzz, the area ratio, A_0/A_3, is rather high and the shock is moved upstream, resulting in a drastic reduction of the plenum pressure. This is due to the boundary layer growth and/or the flow separation at the inlet lip and in the diffuser. At this point, the shock stops for a short time, causing A_0/A_3 to become constant. Thus, the discharge period terminates. A qualitative curve for the actual buzz is presented in Fig. 20. During the calculation, the following assumptions were made:

$M_0 = 2.0$ $\qquad$ $A_5/A_4 = .4$

$A_3/A_4 = .5$ $\qquad$ $\gamma = 1.4$

3.1.3b Fill-Up Period

During the fill-up period, the normal shock is allowed to the diff Therefore, the flow condition n is ent to the upstream flow condition as shown in Fig. 19. Then, Eqn.(3.1-55) becomes:

$$m_3=\frac{gA_3P_{t_3}}{a_{t_3}}\gamma M_3\left\{1+\frac{\gamma-1}{2}M_3^2\right\}^{-\frac{(\gamma+1)}{2(\gamma-1)}}=\frac{gA_3P_{t_0}}{a_{t_0}}\gamma M_0\left\{1+\frac{\gamma-1}{2}M_0^2\right\}^{-\frac{(\gamma+1)}{2(\gamma-1)}} \quad (3.1\text{-}68)$$

On the other hand, the exit mass flow, Eqn.(3.1-56), is also valid in this case.

$$m_5=g\frac{A_5P_{t_5}}{a_{t_5}}\gamma\left\{\frac{\gamma+1}{2}\right\}^{-\frac{(\gamma+1)}{2(\gamma-1)}}=g\frac{A_5P_{t_4}}{a_{t_0}}\gamma\left\{\frac{\gamma+1}{2}\right\}^{-\frac{(\gamma+1)}{2(\gamma-1)}} \quad (3.1\text{-}69)$$

where, $P_{t_4}=P_{t_5}$

$$a_{t_5}=\sqrt{\gamma gRT_{t_5}}=\sqrt{\gamma gRT_{t_0}}=a_{t_0}$$

Substituting Eqns.(3.1-68) and (3.1-69) into Eqn.(3.1-60), one obtains the following equation:

$$\frac{gA_3P_{t_0}}{a_{t_0}}\gamma M_0\left\{1+\frac{\gamma-1}{2}M_0^2\right\}^{-\frac{(\gamma+1)}{2(\gamma-1)}}-\frac{A_5P_{t_4}}{a_{t_0}}\gamma\left\{\frac{\gamma+1}{2}\right\}^{-\frac{(\gamma+1)}{2(\gamma-1)}}=g\frac{A_4\ell}{a_{t_0}^2}\left(\frac{dP_{t_4}}{dt}\right)$$

where, $a_{t_4}=\sqrt{\gamma gRT_{t_4}}=\sqrt{\gamma gRT_{t_0}}=a_{t_0}$

The above formula can be simplified and non-dimensionalized as follows:

$$\frac{a_{t_0}\gamma}{\ell}\left[\frac{A_3}{A_4}M_0\left\{1+\frac{\gamma-1}{2}M_0^2\right\}^{-\frac{(\gamma+1)}{2(\gamma-1)}}-\frac{A_5}{A_4}\left\{\frac{\gamma+1}{2}\right\}^{-\frac{(\gamma+1)}{2(\gamma-1)}}\frac{P_{t_4}}{P_{t_0}}\right]=\frac{d\left(\frac{P_{t_4}}{P_{t_0}}\right)}{dt} \quad (3.1\text{-}70)$$

This equation can be solved exactly. Eqn.(3.1-70) can be re-written as:

$$K\left(C_3-C_4\frac{P_{t_4}}{P_{t_0}}\right)=\frac{d\left(\frac{P_{t_4}}{P_{t_0}}\right)}{dt} \quad (3.1\text{-}71)$$

where, $K = \frac{a_{t_0}\gamma}{\ell}$ = constant

$C_3 = \frac{A_3}{A_4} M_0 \left\{1 + \frac{\gamma-1}{2} M_0^2\right\}^{-\frac{(\gamma+1)}{2(\gamma-1)}}$ = non-dimensional constant

$C_4 = \frac{A_5}{A_4} \left\{\frac{\gamma+1}{2}\right\}^{-\frac{(\gamma+1)}{2(\gamma-1)}}$ = non-dimensional constant

Hence,

$$\int K dt = \int \frac{d\left(\frac{P_{t4}}{P_{t_0}}\right)}{\left(C_3 - C_4 \frac{P_{t4}}{P_{t_0}}\right)} + C$$

$$Kt = -\frac{1}{C_4} \ln\left(C_3 - C_4 \frac{P_{t4}}{P_{t_0}}\right) + C$$

where, C is a constant of integration.

Suppose $P_{t4} = P_{t4f}$, at $t = 0$. Then,

$$0 = -\frac{1}{C_4} \ln\left(C_3 - C_4 \frac{P_{t4f}}{P_{t_0}}\right) + C$$

$$\therefore C = \frac{1}{C_4} \ln\left(C_3 - C_4 \frac{P_{t4f}}{P_{t_0}}\right)$$

Therefore,

$$Kt = \frac{1}{C_4} \ln\left\{\frac{C_3 - C_4 \frac{P_{t4f}}{P_{t_0}}}{C_3 - C_4 \frac{P_{t4}}{P_{t_0}}}\right\} \qquad (3.1\text{-}72)$$

or

$$C_3 - C_4 \frac{P_{t4}}{P_{t_0}} = \left(C_3 - C_4 \frac{P_{t4f}}{P_{t_0}}\right) e^{-C_4 K t}$$

Thereore,

$$\frac{P_{t4}}{P_{t_0}} = \frac{C_3}{C_4} - \left(\frac{C_3}{C_4} - \frac{P_{t4f}}{P_{t_0}}\right) e^{-C_4 Kt} \qquad (3.1\text{-}73)$$

where, $Kt = \frac{a_{t_0}\gamma}{\ell}\, t$ =non-dimensional constant

$C_3 = \frac{A_3}{A_4} M_0 \left\{1 + \frac{\gamma-1}{2} M_0^2\right\}^{-\frac{(\gamma+1)}{2(\gamma-1)}}$ =non-dimensional constant

$C_4 = \frac{A_5}{A_4}\left\{\frac{\gamma+1}{2}\right\}^{-\frac{(\gamma+1)}{2(\gamma-1)}}$ =non-dimensional constant

Calculation results of Eqn.(3.1-73) are shown in Fig.21. It should be noted that in actual engines of supersonic aircrafts, the nozzle exit Mach number is unity and the diffuser throat Mach number is a function of the flight Mach number, Mo, and the ratio of the diffuser throat area, A_3, to the inlet lip area, A_2. In the present case, $A_2/A_3 = 1$.

Consider a rate of the plenum pressure build-up during the fill-up period as a function of M_3. Applying Fig. 19 to the present case,

$$M_3 = M_2 = M_0 \qquad (3.1\text{-}74)$$

From Eqn.(3.1-70),

$$\frac{a_{t_0}\gamma}{\ell}\left[P_{t_0}\frac{A_3}{A_4} M_0\left\{1 + \frac{\gamma-1}{2} M_0^2\right\}^{-\frac{(\gamma+1)}{2(\gamma-1)}} - P_{t4}\frac{A_5}{A_4}\left\{\frac{\gamma+1}{2}\right\}^{-\frac{(\gamma+1)}{2(\gamma-1)}}\right] = \frac{dP_{t4}}{dt} \qquad (3.1\text{-}75)$$

Since

$$a_{t_0} = \sqrt{\gamma g R T_{t_0}} = \sqrt{\gamma g R T_0}\left\{1+\frac{\gamma-1}{2}M_0^2\right\}^{\frac{1}{2}} = a_0\left\{1+\frac{\gamma-1}{2}M_0^2\right\}^{\frac{1}{2}}$$

$$P_{t_0} = P_0\left\{1+\frac{\gamma-1}{2}M_0^2\right\}^{\frac{\gamma}{\gamma-1}}$$

$$P_{t_4} \approx P_4$$

The above formula can be expressed as follows:

$$\frac{a_0\gamma}{\ell}\left\{1+\frac{\gamma-1}{2}M_0^2\right\}^{\frac{1}{2}}\left[P_0\left\{1+\frac{\gamma-1}{2}M_0^2\right\}^{\frac{\gamma}{\gamma-1}}\frac{A_3}{A_4}M_0\left\{1+\frac{\gamma-1}{2}M_0^2\right\}^{-\frac{(\gamma+1)}{2(\gamma-1)}} - P_4\frac{A_5}{A_4}\left\{\frac{\gamma+1}{2}\right\}^{-\frac{(\gamma+1)}{2(\gamma-1)}}\right] = \frac{dP_{t_4}}{dt}$$

$$\therefore \frac{a_0\gamma}{\ell}\left\{1+\frac{\gamma-1}{2}M_0^2\right\}^{\frac{1}{2}}\left[P_0\frac{A_3}{A_4}M_0\left\{1+\frac{\gamma-1}{2}M_0^2\right\}^{\frac{1}{2}} - P_4\frac{A_5}{A_4}\left\{\frac{\gamma+1}{2}\right\}^{-\frac{(\gamma+1)}{2(\gamma-1)}}\right] = \frac{dP_{t_4}}{dt} \qquad (3.1\text{-}76)$$

Considering Eqn.(3.1-74), one obtains:

$$\frac{\partial\left(\frac{dP_{t_4}}{dt}\right)}{\partial M_3} = P_0\frac{(\gamma-1)}{2}\frac{a_0\gamma}{\ell}\left\{1+\frac{\gamma-1}{2}M_0^2\right\}^{-\frac{1}{2}}M_0\left[2\frac{A_3}{A_4}\frac{1}{M_0}\left\{1+\frac{\gamma-1}{2}M_0^2\right\}^{\frac{1}{2}} \times\left\{1+\frac{3}{2}(\gamma-1)M_0^2\right\} - \frac{P_4}{P_0}\frac{A_5}{A_4}\left(\frac{\gamma+1}{2}\right)^{-\frac{(\gamma+1)}{2(\gamma-1)}}\right] \qquad (3.1\text{-}77)$$

Since the shock location is unknown, it is impossible to calculate p_4/p_0 accurately. In this paper, it is assumed that the shock exists at Station 4 (see Fig. 19). Therefore,

$$\frac{\partial\left(\frac{dP_{t_4}}{dt}\right)}{\partial M_3} = \mathrm{I}\left(\mathrm{II}-\mathrm{III}\right) \qquad (3.1\text{-}78)$$

where, $I = p_0 \frac{(\gamma-1)}{2} \frac{a_0 \gamma}{\ell} \left\{ 1 + \frac{\gamma-1}{2} M_0^2 \right\}^{-\frac{1}{2}} M_0 > 0 \quad \because M_0 \geq 1$

$$II = 2 \frac{A_3}{A_4} \frac{1}{M_0} \left\{ 1 + \frac{\gamma-1}{2} M_0^2 \right\}^{\frac{1}{2}} \left\{ 1 + \frac{3}{2}(\gamma-1) M_0^2 \right\}, \quad \frac{A_3}{A_4} = .5$$

$$III = \frac{p_4}{p_0} \frac{A_5}{A_4} \left\{ \frac{\gamma+1}{2} \right\}^{-\frac{(\gamma+1)}{2(\gamma-1)}}, \quad \frac{A_5}{A_4} = .4$$

Then from the results of the numerical calculation shown in Fig. 23, it can be seen that the rate of the plenum pressure build-up increases with increasing M_3, which in the present case is equal to the flight Mach number M_0. It is also shown in Fig. 23 that the rate of the plenum pressure build-up, $\frac{dP_{t_4}}{dt}$, is a function of the flight Mach number, M_0. This curve is based on Eqn.(3.1-76) and indicates that the plenum pressure is built up faster at $M_3 > 1$ than at $M_3 = 1$. This tendency agrees with Dailey's observation.

The final plenum pressure during the fill-up period is obtained from Eqn.(3.1-73).

$$\left(\frac{P_{t_4}}{P_{t_0}} \right)_{t \to \infty} = \frac{C_3}{C_4} = \frac{A_3}{A_5} M_0 \left\{ \frac{1 + \frac{\gamma-1}{2} M_0^2}{\frac{\gamma+1}{2}} \right\}^{-\frac{(\gamma+1)}{2(\gamma-1)}} \qquad (3.1\text{-}79)$$

This shows that the final plenum pressure during the fill-up period is only a function of the flight Mach number and the diffuser geometry, and not a function of the initial plenum pressure of the discharge period. Therefore, if the final plenum pressure is higher than the initial plenum pressure, the buzz phenomenon is likely to occur periodically. On the other hand, if the final plenum pressure is lower than the initial plenum pressure, the buzz stops after one cycle and does not repeat until the external disturbance forces the shock to move upstream to start another buzz cycle.

3.2 HIGH FREQUENCY OSCILLATION

The high frequency oscillation occurs at very low mass flow or even zero mass flow conditions of the supersonic intake diffuser. Under these conditions, the shock is located in front of the inlet lip and the shock movement due to the high frequency oscillation is far smaller than that due to the low frequency oscillation. As a result, the acoustic and aerodynamic characteristics of the intake are less dependent on the geometrical configuration. In this report, a theory of the characteristics of the high frequency oscillation is shown for a simple open nose inlet diffuser (see Fig. 4). This theory is obtained from Ref.13. The flow behind the shock is subsonic and diffuses continuously through the intake diffuser. If the diffuser area does not change drastically, the flow may be considered as quasi-one-dimensional. In order to further simplify this problem, the following assumptions were made:

1. Flow is non-viscous and thermodynamically perfect.

2. Change of the flow area in the duct is so small that it is treated as if it were a constant area duct.

3. Area contraction at the exit nozzle is abrupt. Therefore there is no time delay in the pressure and velocity perturbations between Stations 4 and 5.

4. Neither compressor nor combustion chamber is installed in the duct.

The basic equations in the constant area duct from Station 2 to Station 42 in Fig. 4 are:

$$\frac{\partial \rho}{\partial t} + \frac{\partial}{\partial x}(\rho u) = 0 \qquad \text{(continuity)} \qquad (3.2\text{-}1)$$

$$\frac{\partial(\rho u)}{\partial t} + \frac{\partial}{\partial x}(\rho u^2) = -\frac{\partial p}{\partial x}$$

or:

$$\frac{\partial u}{\partial t} + u\frac{\partial u}{\partial x} = -\frac{1}{\rho}\frac{\partial p}{\partial x} = -\gamma\frac{p}{\rho^2}\frac{\partial \rho}{\partial x} = -\frac{a^2}{\rho}\frac{\partial \rho}{\partial x}$$

(momentum) (3.2-2)

If the velocity, u, and the density, ρ, have solutions of the form,

$$\left.\begin{aligned} u &= \bar{u} + u' = \bar{u}(1 + \nu e^{(\alpha+i\omega)t}) \\ \rho &= \bar{\rho} + \rho' = \bar{\rho}(1 + \sigma e^{(\alpha+i\omega)t}) \end{aligned}\right\} \qquad (3.2\text{-}3)$$

where, $\bar{u}$ and $\bar{\rho}$ = mean velocity and mean density

u' and ρ' = perturbed velocity and perturbed density, and $u' \ll \bar{u}$, $\rho' \ll \bar{\rho}$

ν and σ = functions of x

ω = angular frequency

α = constant

If, $\alpha > 0$, u' and ρ' increase with increasing time, t. Similarly, if $\alpha < 0$, u' and ρ' decrease with increasing time. Substituting Eqn.(3.2-3) into Eqns.(3.2-1) and (3.2-2), the following equations are obtained:

$$\frac{d\nu}{dx} + \frac{d\sigma}{dx} + \frac{\alpha + i\omega}{u}\sigma = 0 \qquad (3.2\text{-}4)$$

$$\frac{\alpha + i\omega}{\bar{u}}\nu + \frac{d\nu}{dx} + \frac{a^2}{\bar{u}}\frac{d\sigma}{dx} = 0 \qquad (3.2\text{-}5)$$

Solving the above simultaneous equations, one obtains:

$$\nu = C_1 e^{\frac{\alpha+i\omega}{1-M}\cdot\frac{x}{a}} + C_2 e^{-\frac{\alpha+i\omega}{1+M}\cdot\frac{x}{a}} \qquad (3.2\text{-}6)$$

$$\sigma = -C_1 M e^{\frac{\alpha+i\omega}{1+M}\cdot\frac{x}{a}} + C_2 M e^{-\frac{\alpha+i\omega}{1+M}\cdot\frac{x}{a}} \qquad (3.2\text{-}7)$$

The first terms of the right hand side of Eqns. (3.2-6) and (3.2-7) represent a wave travelling upstream with a speed of (1-M)a, i.e. with an acoustic speed relative to the air flow. The second terms represent a wave travelling downstream with a speed of (1+M)a. In the above equations, C_1 and C_2 are constants which should be determined from the boundary conditions.

From assumption 3, the contraction of the exit nozzle is so abrupt that there is no time delay in the flow fluctuation between the duct end and the exit nozzle. Under this assumed condition, the steady gasdynamics relationships hold.

$$\rho_{42} A_{42} u_{42} = \rho_5 A_5 u_5 \qquad \text{(continuity)} \qquad (3.2\text{-}8)$$

$$T_{42} + \frac{u_{42}^2}{2C_p g J} = T_5 + \frac{u_5^2}{2C_p g J} \qquad \text{(energy)} \qquad (3.2\text{-}9)$$

Since an isentropic flow is assumed between these two locations,

$$\frac{T_5}{T_{42}} = \left(\frac{\rho_5}{\rho_{42}}\right)^{\gamma-1} \qquad (3.2\text{-}10)$$

From Eqns.(3.2-9) and (3.2-10)

$$T_{42} = T_5 \left(\frac{\rho_{42}}{\rho_5}\right)^{\gamma-1}$$

$$\therefore \; T_5\left\{1-\left(\frac{\rho_{42}}{\rho_5}\right)^{\gamma-1}\right\} = \frac{1}{2C_p g J}(u_{42}^2 - u_5^2) = \frac{u_{42}^2}{2C_p g J}\left\{1-\left(\frac{u_5}{u_{42}}\right)^2\right\}$$

Combining the above formula with Eqn.(3.2-8), the following equation is obtained:

$$\frac{u_{42}^2}{2C_p g J T_5} = \frac{1-\left(\frac{\rho_{42}}{\rho_5}\right)^{\gamma-1}}{1-\left(\frac{u_5}{u_{42}}\right)^2} = \frac{1-\left(\frac{\rho_{42}}{\rho_5}\right)^{\gamma-1}}{1-\left(\frac{\rho_{42}}{\rho_5}\right)^2\left(\frac{A_{42}}{A_5}\right)^2} \qquad (3.2\text{-}11)$$

Substituting Eqn.(3.2-3) into Eqn.(3.2-11), and neglecting the second and higher order terms, one obtains:

$$\nu = \frac{\left(1+\frac{\gamma-1}{2}M_5^2\right) - M_5^2\left(1+\frac{\gamma-1}{2}M_4^2\right)}{M_5^2 - M_4^2}\,\sigma \qquad (3.2\text{-}12)$$

where, M_4 is assumed to be equal to M_{42}.

Since the flow Mach number at the nozzle exit is unity

under the actual supersonic flight condition, $M_5=1$. Then one obtains:

$$\nu = \left(\frac{\gamma-1}{2}\right)\sigma \tag{3.2-13}$$

If the flow at the inlet is assumed to enter the duct from a plenum chamber, Eqn.(3.2-12) is still useful provided M_5 is replaced by 0. Then,

$$\nu = -\frac{1}{M_4^2}\sigma \tag{3.2-14}$$

At the inlet, however, by definition, x = 0. Therefore, combining Eqns.(3.2-6) and (3.2-7) into Eqn.(3.2-14), one obtains:

$$\nu = C_1 + C_2 = -\frac{1}{M_4^2}\sigma = -\frac{1}{M_4^2}(-C_1 M_4 + C_2 M_4)$$

$$\therefore\ C_1 + C_2 = -\frac{1}{M_4}(-C_1 + C_2)$$

Therefore,

$$\frac{C_1}{C_2} = \frac{1+M_4}{1-M_4} \tag{3.2-15}$$

Also, at the exit, where $x = \ell$, the following relationships are obtained:

$$\nu = C_1 e^{\frac{\alpha+i\omega}{1-M_4}\cdot\frac{\ell}{a}} + C_2 e^{-\frac{\alpha+i\omega}{1+M_4}\cdot\frac{\ell}{a}} = \left(\frac{\gamma-1}{2}\right)\sigma = \left(\frac{\gamma-1}{2}\right)\left(-C_1 M_4 e^{\frac{\alpha+i\omega}{1-M_4}\cdot\frac{\ell}{a}}\right.$$

$$\left. + C_2 M_4 e^{-\frac{\alpha+i\omega}{1+M_4}\cdot\frac{\ell}{a}}\right) = \left(\frac{\gamma-1}{2}\right)\left(-C_1 M_4 e^{\frac{\alpha+i\omega}{1-M_4}\cdot\frac{\ell}{a}} + C_2 M_4 e^{-\frac{\alpha+i\omega}{1+M_4}\cdot\frac{\ell}{a}}\right) \tag{3.2-16}$$

From Eqns.(3.2-15) and (3.2-16),

$$\frac{1+M_4}{1-M_4}e^{\frac{\alpha+i\omega}{1-M_4}\cdot\frac{\ell}{a}}+e^{-\frac{\alpha+i\omega}{1+M_4}\cdot\frac{\ell}{a}}=M_4\left(\frac{\gamma-1}{2}\right)\left(-\frac{1+M_4}{1-M_4}e^{\frac{\alpha+i\omega}{1-M_4}\cdot\frac{\ell}{a}}+e^{-\frac{\alpha+i\omega}{1+M_4}\cdot\frac{\ell}{a}}\right)$$

$$\frac{1+M_4}{1-M_4}e^{\frac{\alpha+i\omega}{1-M_4^2}\cdot\frac{2\ell}{a}}+1=M_4\left(\frac{\gamma-1}{2}\right)\left(-\frac{1+M_4}{1-M_4}e^{\frac{\alpha+i\omega}{1-M_4^2}\cdot\frac{2\ell}{a}}+1\right)$$

$$\therefore\ e^{\frac{\alpha+i\omega}{1-M_4^2}\cdot\frac{2\ell}{a}}=-\frac{(1-M_4)\left\{1-\left(\frac{\gamma-1}{2}\right)M_4\right\}}{(1+M_4)\left\{1+\left(\frac{\gamma-1}{2}\right)M_4\right\}} \qquad (3.2\text{-}17)$$

Therefore,

$$\left.\begin{aligned} e^{\frac{2\alpha\ell}{a(1-M_4^2)}}\cos\frac{2\omega\ell}{a(1-M_4^2)} &= -\frac{(1-M_4)\left\{1-\left(\frac{\gamma-1}{2}\right)M_4\right\}}{(1+M_4)\left\{1+\left(\frac{\gamma-1}{2}\right)M_4\right\}} \\ e^{\frac{2\alpha\ell}{a(1-M_4^2)}}\sin\frac{2\omega\ell}{a(1-M_4^2)} &= 0 \end{aligned}\right\} \qquad (3.2\text{-}18)$$

Since the flow Mach number in the duct is subsonic,

$$0\le M_4<1 \qquad (3.2\text{-}19)$$

Then, for air using $\gamma = 1.4$, the following expression is obtained:

$$-\frac{(1-M_4)\left(1-\frac{\gamma-1}{2}M_4\right)}{(1+M_4)\left(1+\frac{\gamma-1}{2}M_4\right)}<0 \qquad (3.2\text{-}20)$$

From Eqn.(3.2-18),

$$\left.\begin{aligned} &\frac{2\omega\ell}{a(1-M_4^2)} = (2n-1)\pi \quad (>0) \\ &\text{where, } n = 1, 2, 3, \ldots\ldots \\ &\text{and} \\ &e^{\frac{2\alpha\ell}{a(1-M_4^2)}} = \frac{(1-M_4)(1-\frac{\gamma-1}{2}M_4)}{(1+M_4)(1+\frac{\gamma-1}{2}M_4)} \end{aligned}\right\} \qquad (3.2\text{-}21)$$

The frequency, f, is defined as:

$$f = \frac{\omega}{2\pi}$$

$$\therefore\ f = \frac{1}{2\pi}\frac{a(1-M_4^2)}{2\ell}(2n-1)\pi = \frac{(2n-1)}{4}\frac{a}{\ell}(1-M_4^2) \qquad (3.2\text{-}22)$$

It can be seen that the frequency reduces with increasing flow Mach number, provided that the acoustic speed, a, is constant. Results of Eqn.(3.2-22) are shown in Fig. 24. When $M_4 = 0$, the frequency reduces to the simple organ pipe oscillation.

When considering the damping characteristics of such oscillations, a logarithmic decrement, δ, may be defined as:

$$\delta = \ln\frac{e^{\alpha t}}{e^{\alpha(t+\tau)}} = -\frac{2\pi\alpha}{\omega} \qquad (3.2\text{-}23)$$

where, τ = period of oscillation.

It is obvious that when $\alpha < 0$, the fluctuation is damped. From Eqn.(3.2-21),

$$\delta = -\frac{2\pi\alpha}{\omega} = -\frac{2}{(2n-1)} \ln \frac{(1-M_4)\left(1-\frac{\gamma-1}{2}M_4\right)}{(1+M_4)\left(1+\frac{\gamma-1}{2}M_4\right)}$$

or:

$$\delta = \frac{2}{2n-1} \ln \frac{(1+M_4)\left(1+\frac{\gamma-1}{2}M_4\right)}{(1-M_4)\left(1-\frac{\gamma-1}{2}M_4\right)} \qquad (3.2\text{-}24)$$

This curve is presented in Fig. 25. The family of curves indicates that δ is positive, independent of the mode "n" and Mach number of the flow. However, it can be seen from these analytical results that at a certain free stream Mach number, an oscillation corresponding to a lower mode "n" will experience a higher damping factor or vice versa. This finding agrees with Dailey's test results.

Although this analysis provides a reasonable qualitative solution, there are many additional points which would require further consideration:

1. This theory does not indicate which mode of oscillation would occur under a given condition. Actually, the mode of oscillation observed varies with the mass flow rate.

2. This theory neglects the shock which is located in front of the diffuser inlet lip. This will lead to serious errors because high frequency flow oscillations do not

occur in a subsonic intake diffuser where no shock exists.

3. As a boundary condition, the diffuser inlet flow Mach number is assumed to be zero. This simplification is questionable, since the flow entering the diffuser must have a finite flow Mach number. Even though there is a small gap between the diffuser inlet and the shock, this cannot logically be simulated by a plenum chamber except at the take-off condition in which the mass flow is very high and the flight velocity is nearly zero.

With the limitations offered by the present theory on high frequency oscillation phenomenon as a result of the aforementioned simplifications, it is felt that further studies on the acoustic/shock wave interactions should be carried out in order to achieve a better understanding of this highly complex problem.

4. CONCLUDING REMARKS

From previous investigations and the present theoretical analysis, the following conclusions can be drawn:

1. Low Frequency Oscillation

   a. It is shown in the present analysis that a possibility exists for the buzz to be initiated by a disturbance, propagated either from the upstream or downstream of the shock. According to Dailey and Trimpi, the disturbance, if it exists, must be generated only upstream of the inlet lip.

   b. Once the shock starts moving upstream from the initial subcritical position, the mass flow reduces. This results in the higher static pressure rise between the shock and the inlet lip, and possibly causes the sudden increases in boundary layer thickness and flow separation on the center body of a spike diffuser. The resultant reduction of the effective flow area at the inlet lip further limits the inlet mass flow and the shock is pushed further upstream.

c. When the exit mass flow rate is higher than that of the in-flow, pressure starts to reduce in the plenum chamber. The plenum pressure of an open nose intake diffuser during this discharge period of the buzz is developed in this report and shown by the following

$$\frac{P_{t4}}{P_{t0}} = \left(\frac{P_{t4'}}{P_{t0}}\right) e^{(C_1 - C_2)Kt}$$

where, $Kt = \frac{a_{t0}\,\gamma}{\ell}\,t$ =non-dimensional constant

$C_1 = \frac{A_3}{A_4} M_3 \left\{1 + \frac{(\gamma-1)}{2} M_3^2\right\}^{-\frac{(\gamma+1)}{2(\gamma-1)}}$ =non-dimensional constant

$C_2 = \frac{A_5}{A_4}\left\{\frac{\gamma+1}{2}\right\}^{-\frac{(\gamma+1)}{2(\gamma-1)}}$ =non-dimensional constant

Pt = total pressure

$a_{t0} = \sqrt{\gamma g R T_{t0}}$ =acoustic velocity based on total temperature

A = flow area

Subscripts 0,3,4,5 =locations shown in Fig. 4

Subscript 1 =initial condition of the discharge period

The development of this formula employs the simplifying assumptions that both the area ratio, A_0/A_3, and M_3 are constant. The result indicates that the plenum chamber pressure decreases drastically as shown in Fig. 20. Since A_0 is dependent on time and the shock location, and is very difficult of determine analytically, further experimental investigations are required.

d. During the discharge period, the plenum pressure becomes very low and shock is swallowed into the diffuser. When this happens, the mass flow rate increases and the plenum pressure recovers. An equation of the plenum pressure of an open nose intake diffuser during this fill-up period has been developed in this report. This equation has a simple exponential form, as shown below:

$$\frac{P_{t4}}{P_{t0}} = \frac{C_3}{C_4} - \left(\frac{C_3}{C_4} - \frac{P_{t4f}}{P_{t0}}\right) e^{-C_4 K t}$$

where, $Kt = \frac{a_{t0} \cdot \gamma}{\ell} t$ =non-dimensional constant

$$C_3 = \frac{A_3}{A_4} M_0 \left\{1 + \frac{\gamma-1}{2} M_0^2\right\}^{-\frac{(\gamma+1)}{2(\gamma-1)}}$$ =non-dimensional constant

$$C_4 = \frac{A_5}{A_4} \left\{\frac{\gamma+1}{2}\right\}^{-\frac{(\gamma+1)}{2(\gamma-1)}}$$ =non-dimensional constant

subscript, f =initial condition of the fill-up period.

This theory is slightly different from Dailey's theory because it considers the diffuser throat Mach number, M_3, to be not only a function of the flight Mach number, M_0, but also the diffuser geometry. It has been proven that as M_3 increases, the plenum pressure builds up more quickly. This tendency agrees with Dailey's observation.

e. Since the shock location is a key in understanding the plenum pressure during the buzz, it is strongly recommended that the behavior of the shock be investigated. Further experimental work is required to provide justification of this theory.

2. High Frequency Oscillation

a. The frequency of the flow oscillation increases when the flow Mach number is reduced. In extreme cases, when the Mach number is zero, the frequency coincides with the organ pipe oscillation.

b. The oscillation has a positive damping characteristic except at the zero flow Mach number. At M = 0, the oscillation has a neutral stability. However, it was found that the damping is less for the higher mode of the oscillation. This finding was further substantiated by Dailey's experimental results.

5. REFERENCES

1. Dailey, C.L. "Supersonic Diffuser Instability", Journal of the Aeronautical Sciences, Vol. 22, No. 11. Nov. 1955.

2. Faro, I.D.V. "Supersonic Inlets", AGARDograph 102, May 1965.

3. Trimpi, R.L. "An Analysis of Buzzing in Supersonic Ram Jets by a Modified One-Dimensional Non-Stationary Wave Theory", NACA RM L52A18, Mar. 1952, Modified to NACA TN 3695, July 1956.

4. Trimpi, R.L. "A Theory for Stability and Buzz Pulsation Amplitude in Ram Jets and an Experimental Investigation Including Scale Effects", NACA RM L53G28.

5. Oswatitsch, K. "Der Druckrückgewinn bei Geschossen mit Rückstossantrieb bei hohen Überschallgeschwichkeiten (Der Wirkungsgrad von Stossdiffusoren). Forschung und Entwicklung des Heereswaffenamtes (Göttingen), Bericht Nr. 1005, 1944.

6. Pearce, R.B. "Causes and Controls of Powerplant Surge", Aviation Week, Vol. 52, No. 3, Jan. 1950.

7. Ferri, A. and Nucci, L.M. "The Origin of Aerodynamic Instability of Supersonic Inlets at Subcritical Conditions", NACA RM L50K30, Jan. 1951.

8. Sterbentz, W.H. and Evvard, J.C. "Criteria for Prediction and Control of Ram-Jet Pulsations, NACA TN3506, Aug. 1955.

9. Chang, C.-C. and Hsu, C.-T. "Aerodynamic Instability of Supersonic Inlet Diffusers", ARS Journal, Vol.30, No. 5, May 1960.

10. Lee, J.H.S. "On the Stability Phenomenon of Supersonic Intake Diffusers", McGill Univ., Technical Note 62-9.

11. Stoolman, L. "Investigation of an Instability Phenomenon in Supersonic Diffusers", CIT PhD Thesis, 1953.

12. Mirels, H. "Acoustic Analysis of Ram-Jet Buzz", NACA TN 3574, Nov. 1955.

13. Whitehead, D.S. "The Vibration of Air in a Duct with a Subsonic Mean Flow", Aeronautical Quarterly, Vol. 12, 1961.

14. Powell, A. "One-Dimensional Treatment of Weak Disturbances for a Shock Wave", A.R.C. Technical Report, C.P. No. 441, 1959.

15. Connors, J.F. and Meyer, R.C. "A Variable-Geometry Annular Cascade-Type Inlet at Mach Numbers of 1.9 and 3.05", NACA RM E56D23a, 1956.

16. Cubbison, R.W., Meleason, E.T. and Johnson, D.F. "Effect of Porous Bleed in a High-Performance, Axisymmetric, Mixed-Compression Inlet at Mach 2.50", NASA TM X-1692, 1968.

17. Sanders, B.W. and Cubbison, R.W. "Effect of Bleed-System Back Pressure and Porous Area on the Performance of an Axisymmetric Mixed-Compression Inlet at Mach 2.50", NASA TM X-1710, 1968.

18. Bowditch, D.N. and Wilcox, F.A. "Dynamic Response of a Supersonic Diffuser to Bypass and Spike Oscillation" NASA TM X-10, 1959.

19. Fraiser, H.R. "Supersonic Inlet Dynamics", Journal of the Aero-Space Sciences, Vol. 27, No. 6, June 1960.

20. Bowditch, D.N., Anderson, B.H. and Tabata, W.K. "Performance and Control of a Full-Scale, Axially Symmetric External-Internal-Compression Inlet from Mach 2.0 to 3.0", NASA TM X-471, 1961.

21. Hurnell, H.G. "Analysis of Shock Motion in Ducts during Disturbances in Downstream Pressure", NACA TN 4090, 1957.

22. Wasserbauer,J.F. and Whipple, D.L. "Experimental Investigation of the Dynamic Response of a Supersonic Inlet to External and Internal Disturnances", NASA TM X-1648, 1966.

23. Verduzio, L. "Research about the Shock Wave Stability in a Supersonic Air-Inlet", Instituto di Macchine e Motori per Aeromobili, Pubblicazione N.87, Sept. 1967.

24. Wasserbauer, J.F. and Willoh, R.G. "Experimental and Analytical Investigation of the Dynamic Response of a Supersonic Mixed-Compression Inlet", AIAA Paper 68-651, June 1968.

25. Willoh, R.G. "A Mathematical Analysis of Supersonic Inlet Dynamics", NASA TN D-4969, 1068.

26. Wasserbauer, J.F. "Dynamic Response of a Mach 2.5 Axisymmetric Inlet with Engine or Cold Pipe and Utilizing Sixty Percent Supersonic Internal Area Contraction", NASA TN D-5338, 1969.

6. ILLUSTRATIONS

FIG.1 SUPERSONIC INTAKE DIFFUSER (SPIKE TYPE)

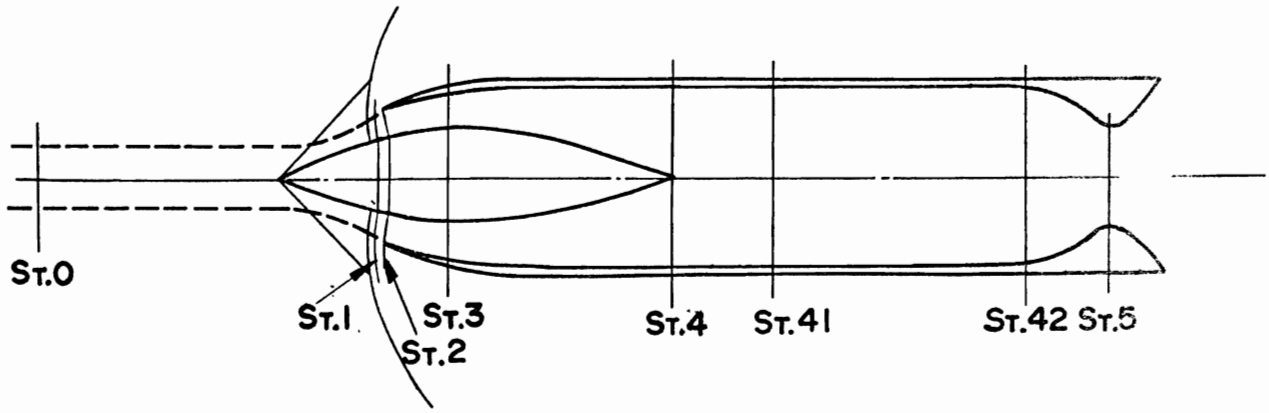

St.0 : INFINITE UPSTREAM
St.1 : DOWNSTREAM OF NORMAL SHOCK
St.2 : INLET LIP
St.3 : DIFFUSER THROAT
St.4 : END OF DIFFUSER
St.41 : COMPRESSOR INLET OR COMBUSTION CHAMBER INLET
St.42: END OF CHAMBER
St. 5 : EXIT THROAT

FIG. 2 SPIKE DIFFUSER (STEADY STATE CONDITION)

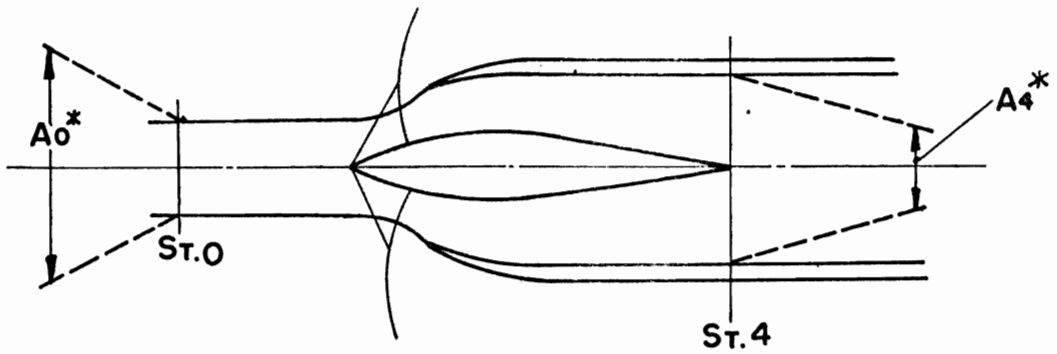

FIG.3 STEADY STATE DIFFUSER CHARACTERISTIC CURVE

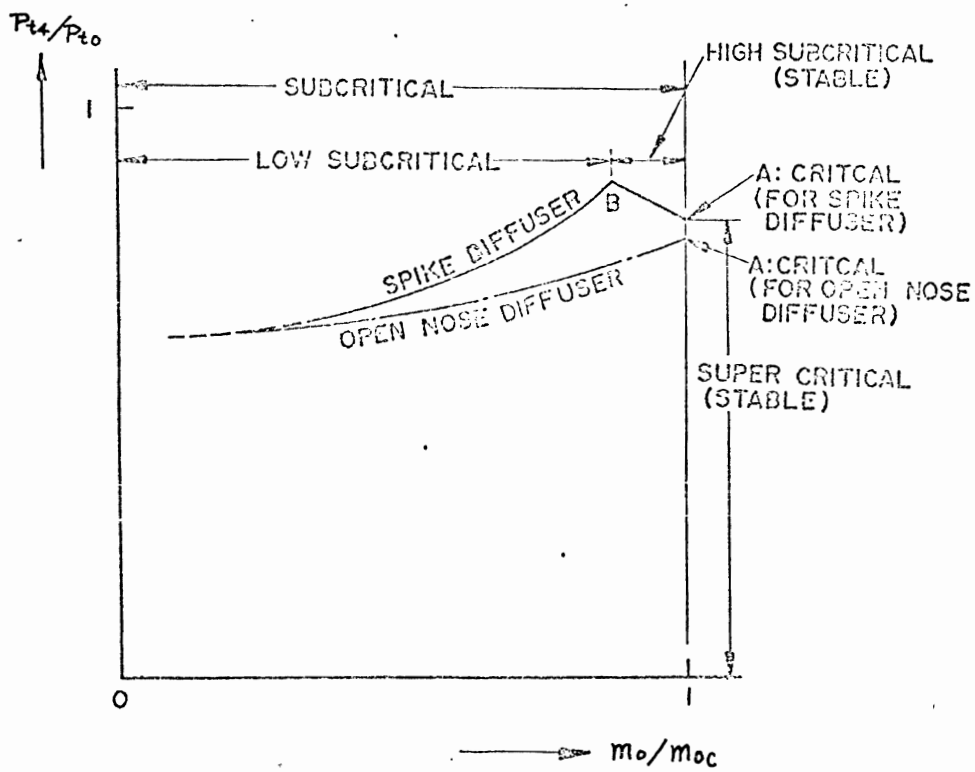

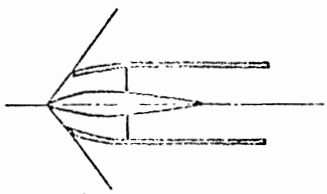

FIG.3A SUPER-CRITICAL CONDITION

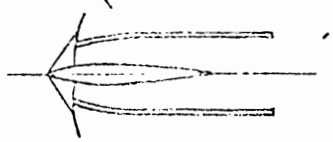

FIG. 3B HIGH SUBCRITICAL CONDITION

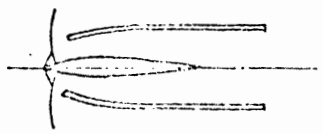

FIG.3C LOW SUBCRITICAL CONDITION

FIG. 4 SUPERSONIC INTAKE DIFFUSER (OPEN NOSE TYPE)

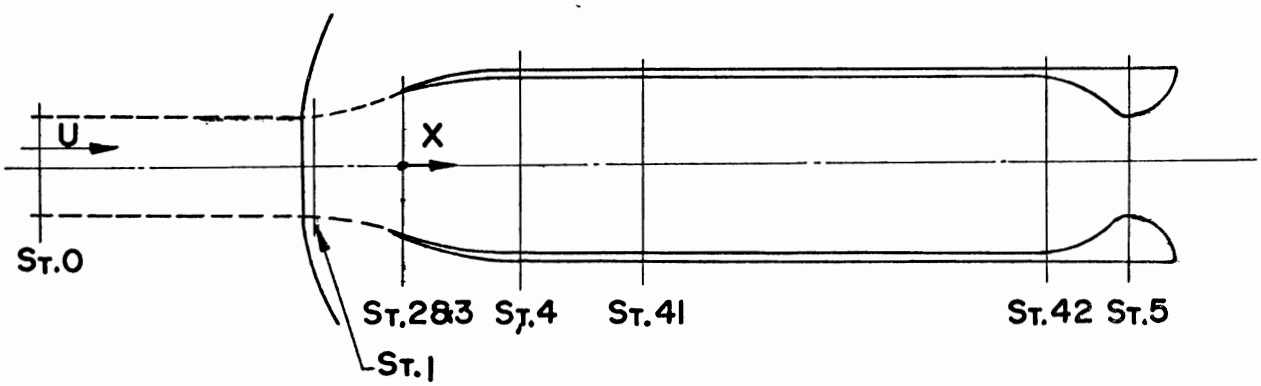

ST.0 : INFINITE UPSTREAM
ST.1 : DOWNSTREAM OF NORMAL SHOCK
ST.2 : INLET LIP
ST.3 : DIFFUSER THROAT
ST.4 : END OF DIFFUSER
ST.41 : COMPRESSOR INLET OR
COMBUSTION CHAMBER INLET
ST.42 : END OF CHAMBER
ST.5 : EXIT THROAT

FIG.5 TYPICAL BUZZ CYCLE (DATA OBTAINED FROM REF.1)

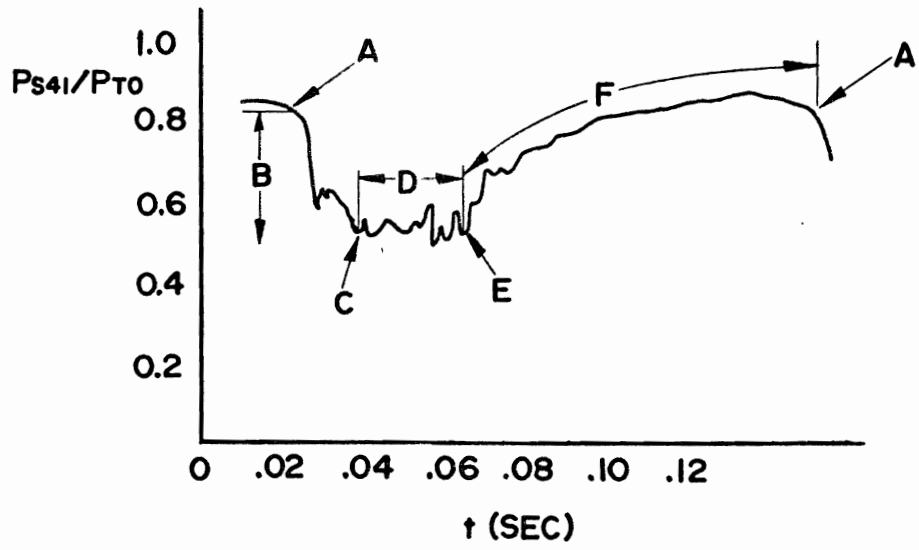

SHOCK LOCATION DURING BUZZ

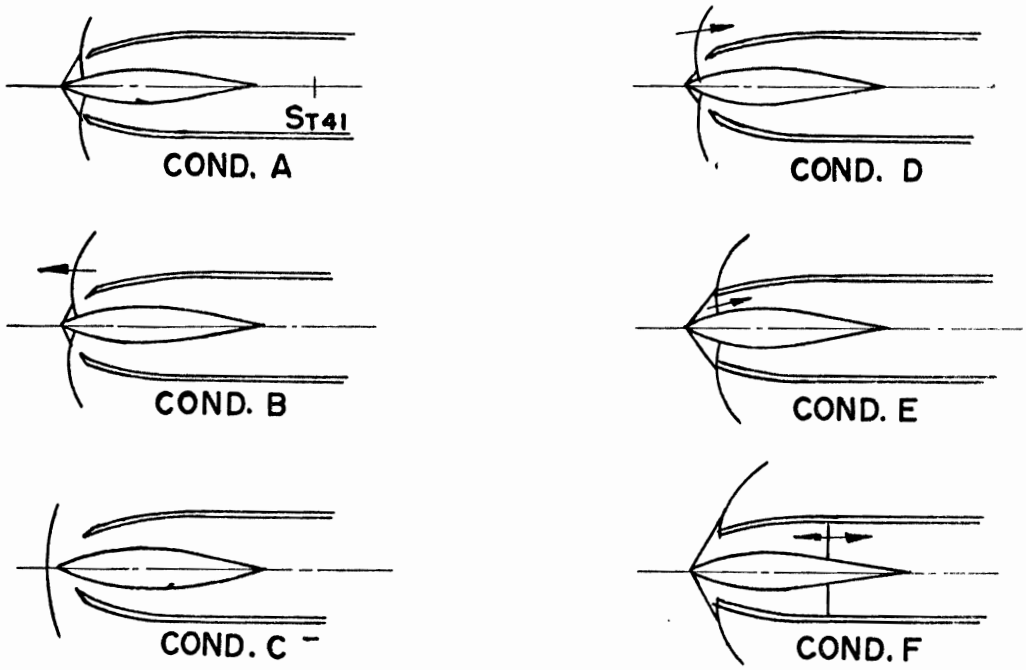

FIG. 6 VORTEX SHEET GENERATED AT SHOCK TRIPLE POINT

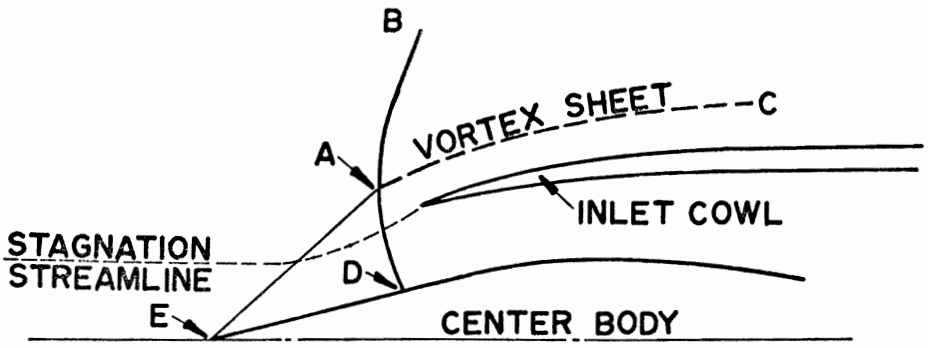

FIG. 6A STEADY CONDITION

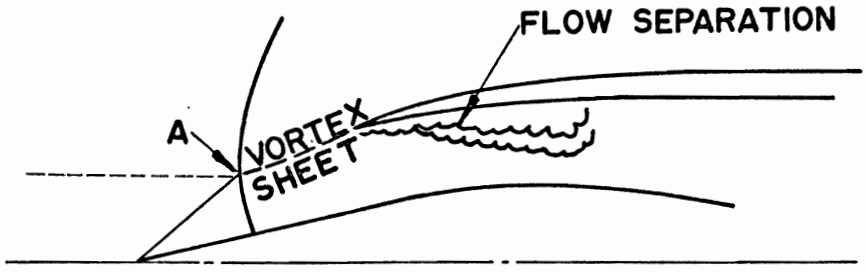

FIG. 6B VORTEX SHEET CAUSES FLOW SEPARATION

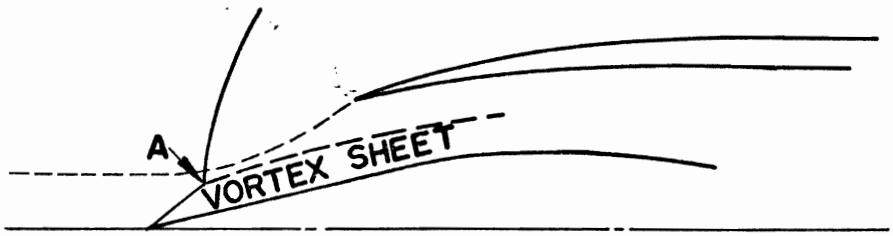

FIG. 6C VORTEX SHEET DETACHES FROM INLET COWL INNER WALL

FIG. 7 VORTEX SHEET GENERATED AT SHOCK TRIPLE POINT AND BOUNDARY LAYER SEPARATION ON CENTER BODY

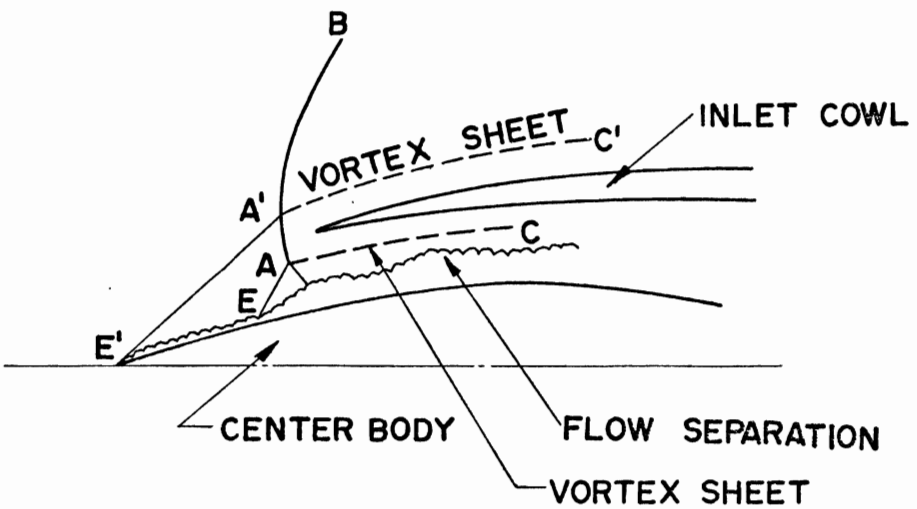

FIG. 8 PRESSURE HISTORY DURING BUZZ
(DATA OBTAINED FROM REF. 1)

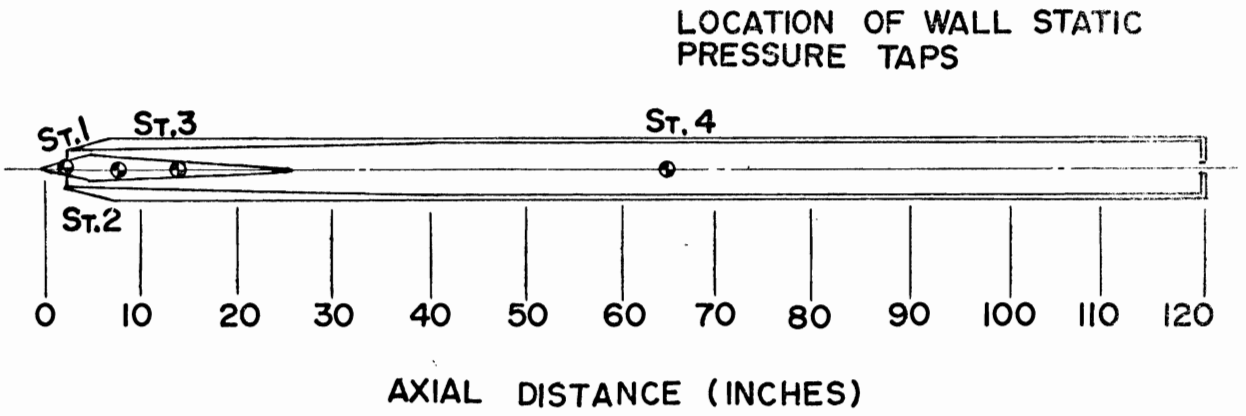

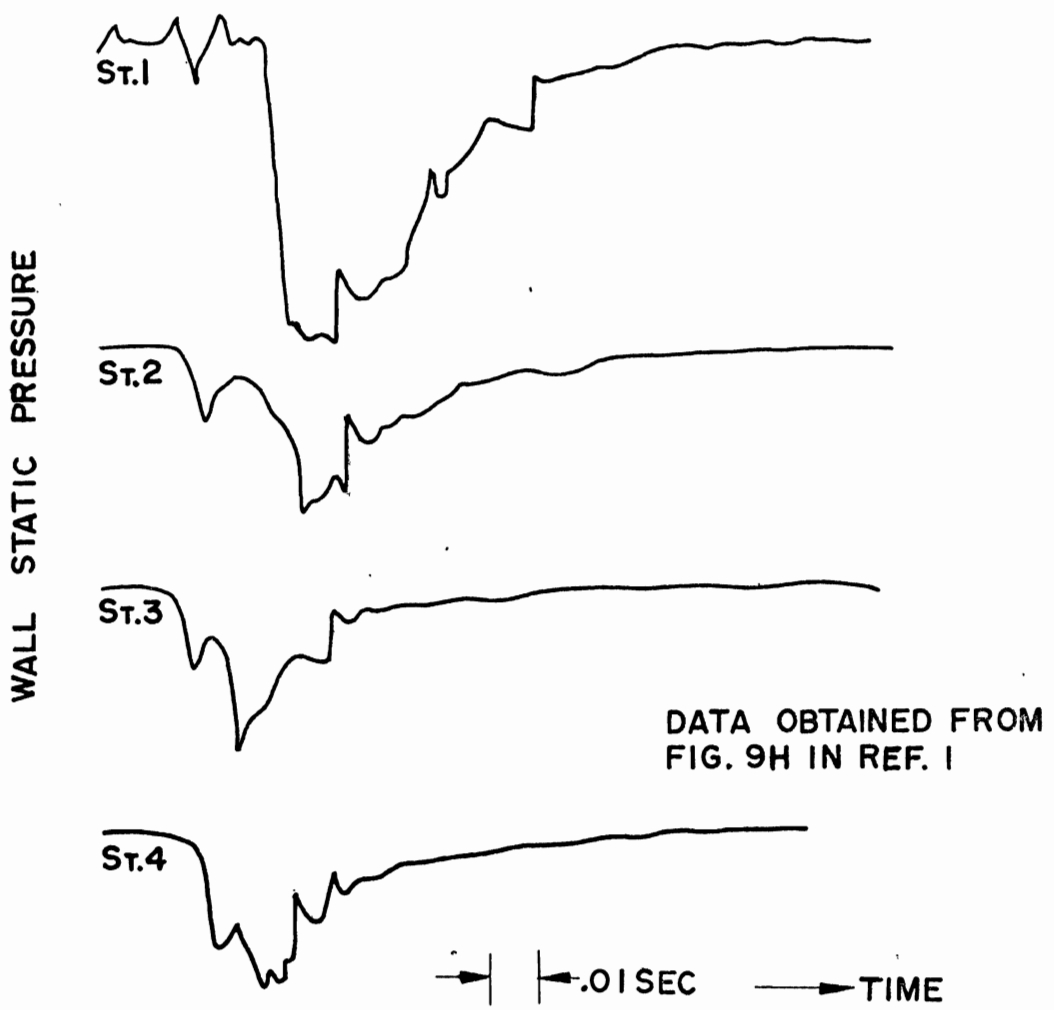

FIG.9 DAILEY'S HYPOTHESIS OF BUZZ INITIATION

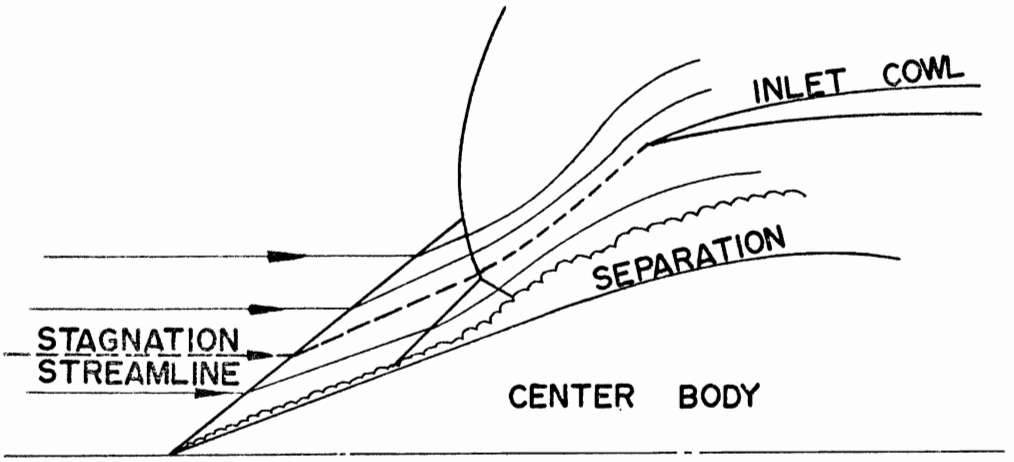

FIG.10 TRIMPI'S HYPOTHETICAL SUPERSONIC INTAKE DIFFUSER

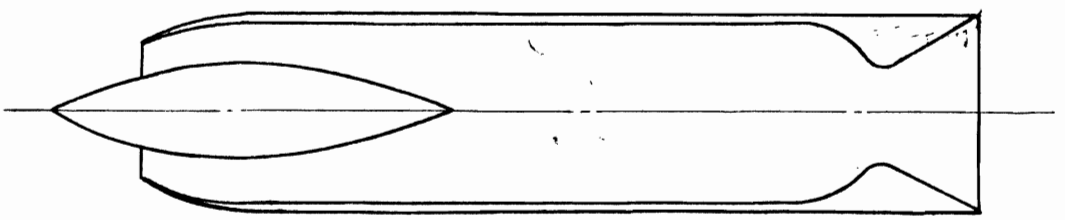

TYPICAL SUPERSONIC INTAKE DIFFUSER
(USED IN TRIMPI'S EXPERIMENT)

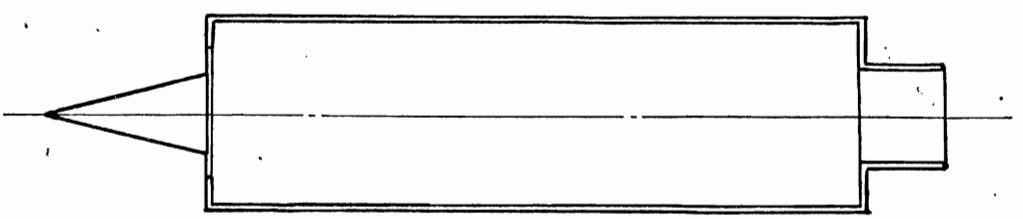

HYPOTHETICAL SUPERSONIC INTAKE DIFFUSER
(USED IN TRIMPI'S THEORETICAL ANALYSIS)

FIG. 11 TRIMPI'S THEORETICAL ANALYSIS (REF. 3)
THEORETICAL PRESSURE HISTORY DURING BUZZ CYCLE

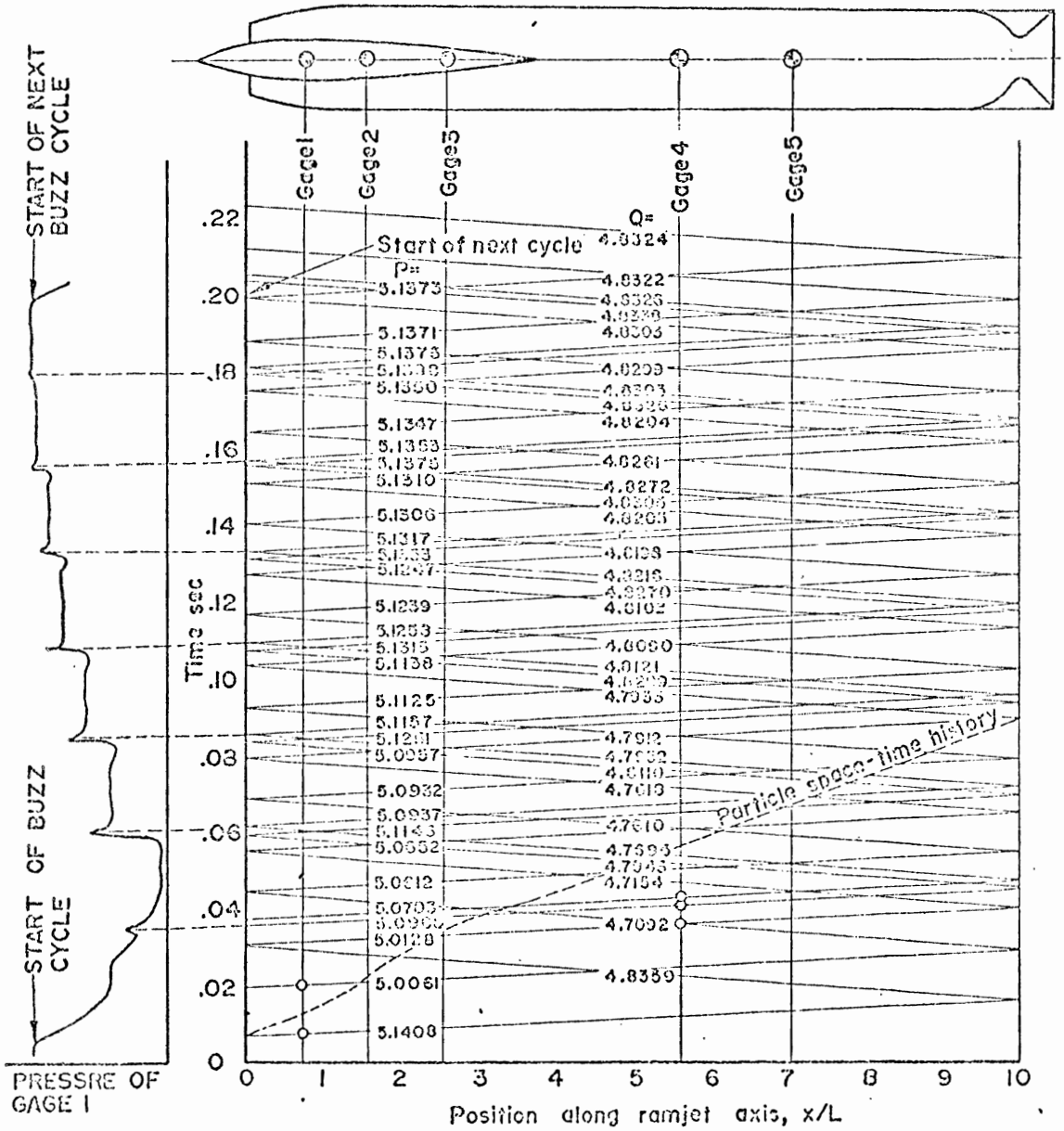

FIG.12 SCHEMATIC VIEW OF PRACTICAL SUPERSONIC INTAKE DIFFUSER (CONVERGENT–DIVERGENT DIFFUSER)

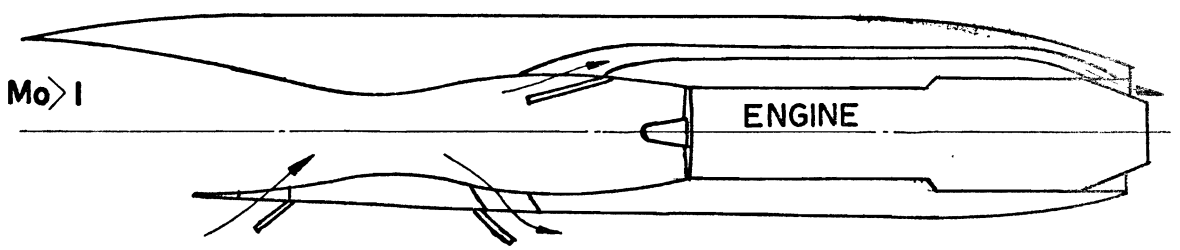

FIG. 13 SUBCRITICAL OPERATION OF SUPERSONIC SPIKE DIFFUSER AND SIMULATED OPEN NOSE DIFFUSER

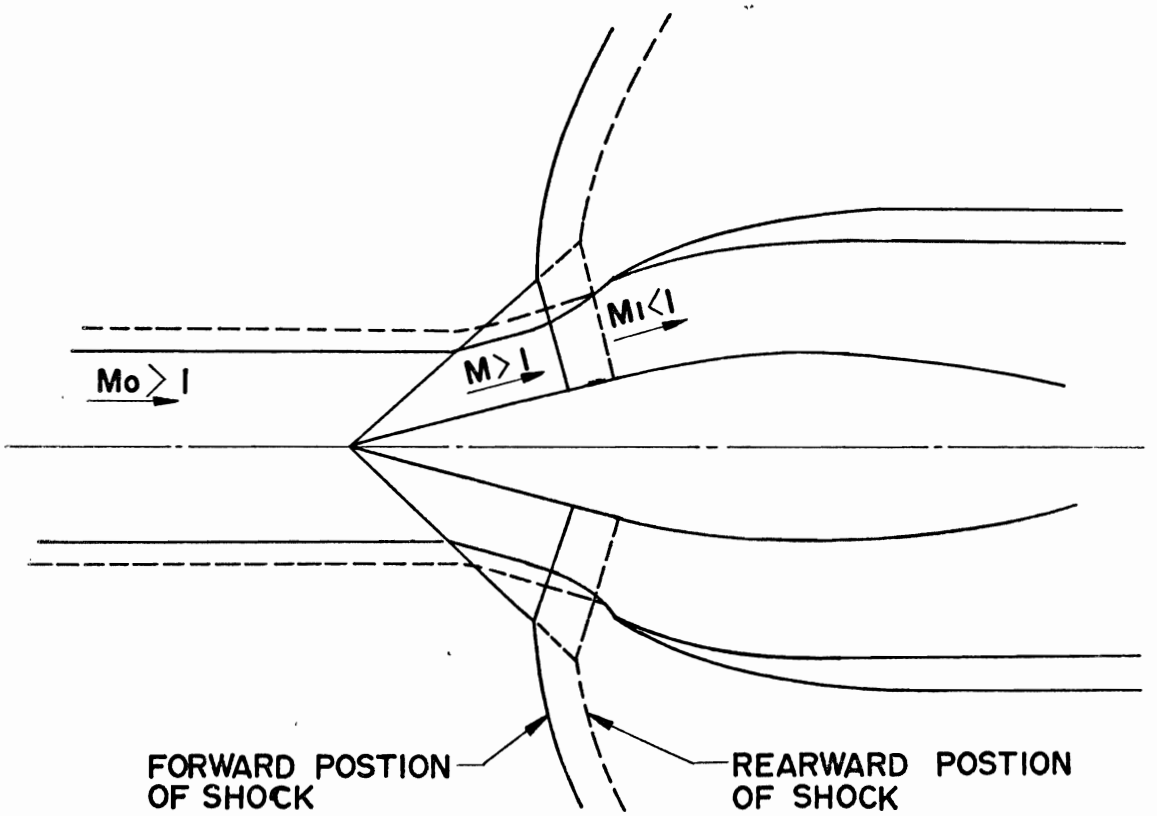

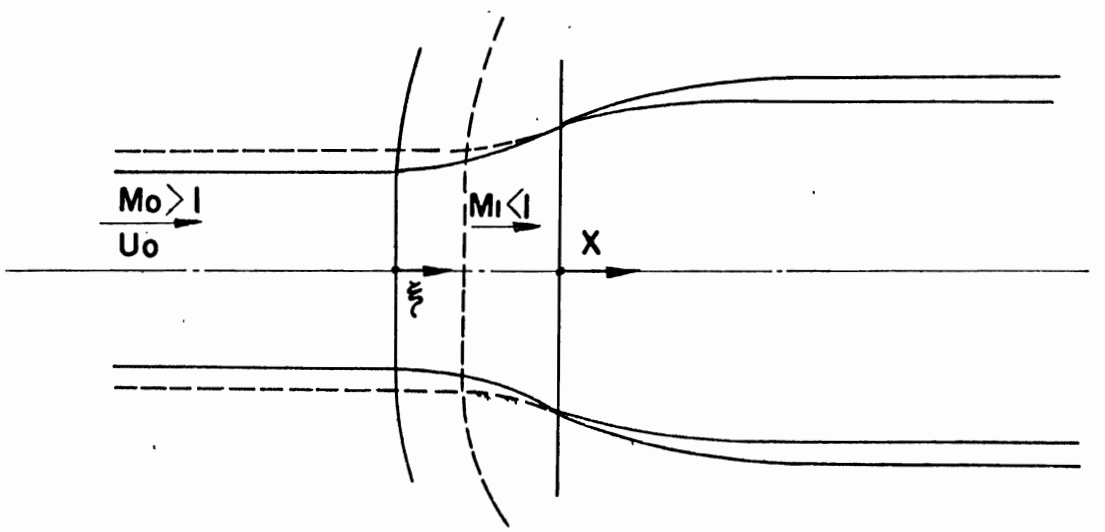

FIG.14 TIME-SPACE DIAGRAM OF SHOCK-DISTURBANCE INTERACTION (DISTURBANCE IS ASSUMED TO BE A COMPRESSION WAVE AND GENERATED IN UPSTREAM OF SHOCK)

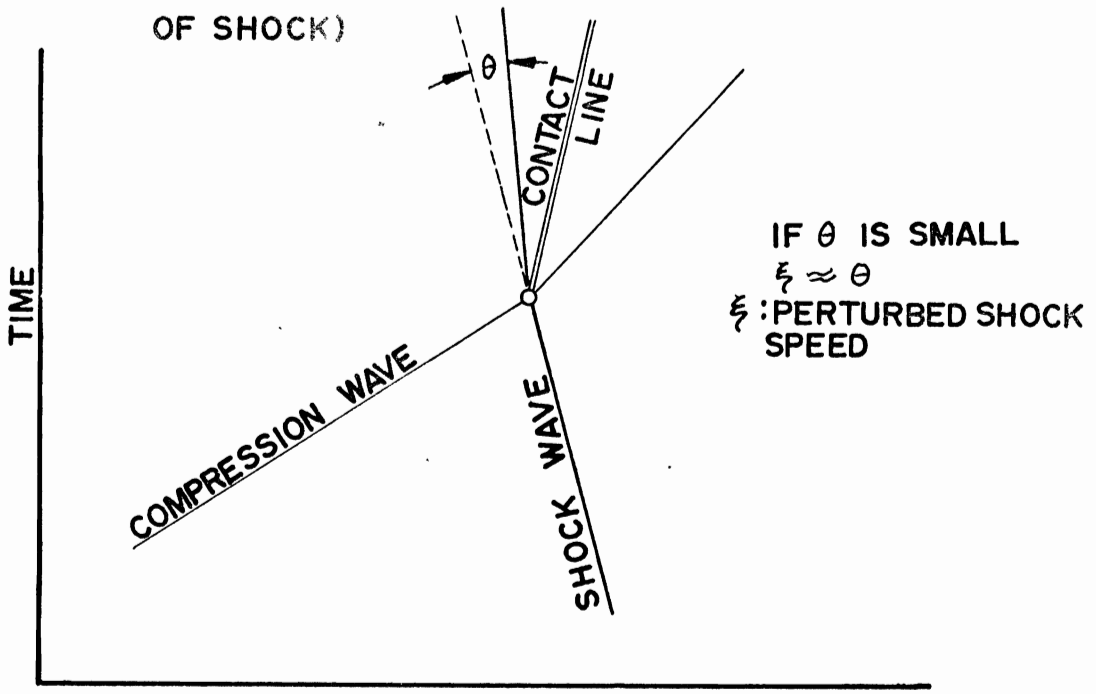

DISTURBANCE COLLIDES HEAD-ON WITH SHOCK

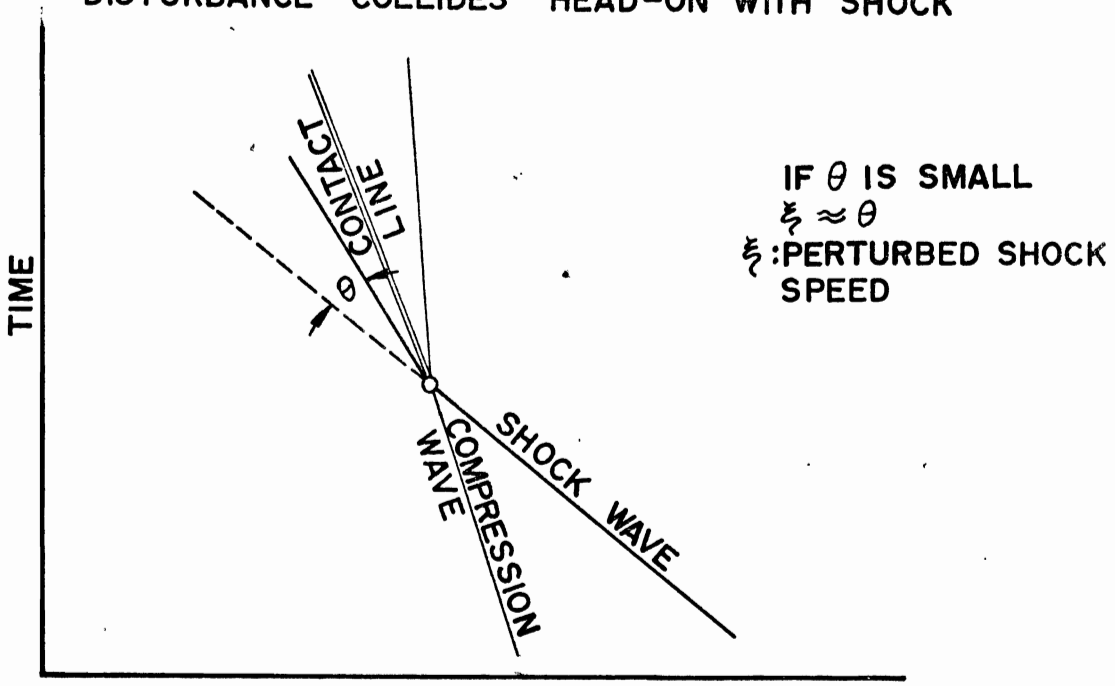

SHOCK CATCHES UP WITH DISTURBANCE

FIG. 15 HEAD ON COLLISION OF PRESSURE PULSE WITH SHOCK WAVE

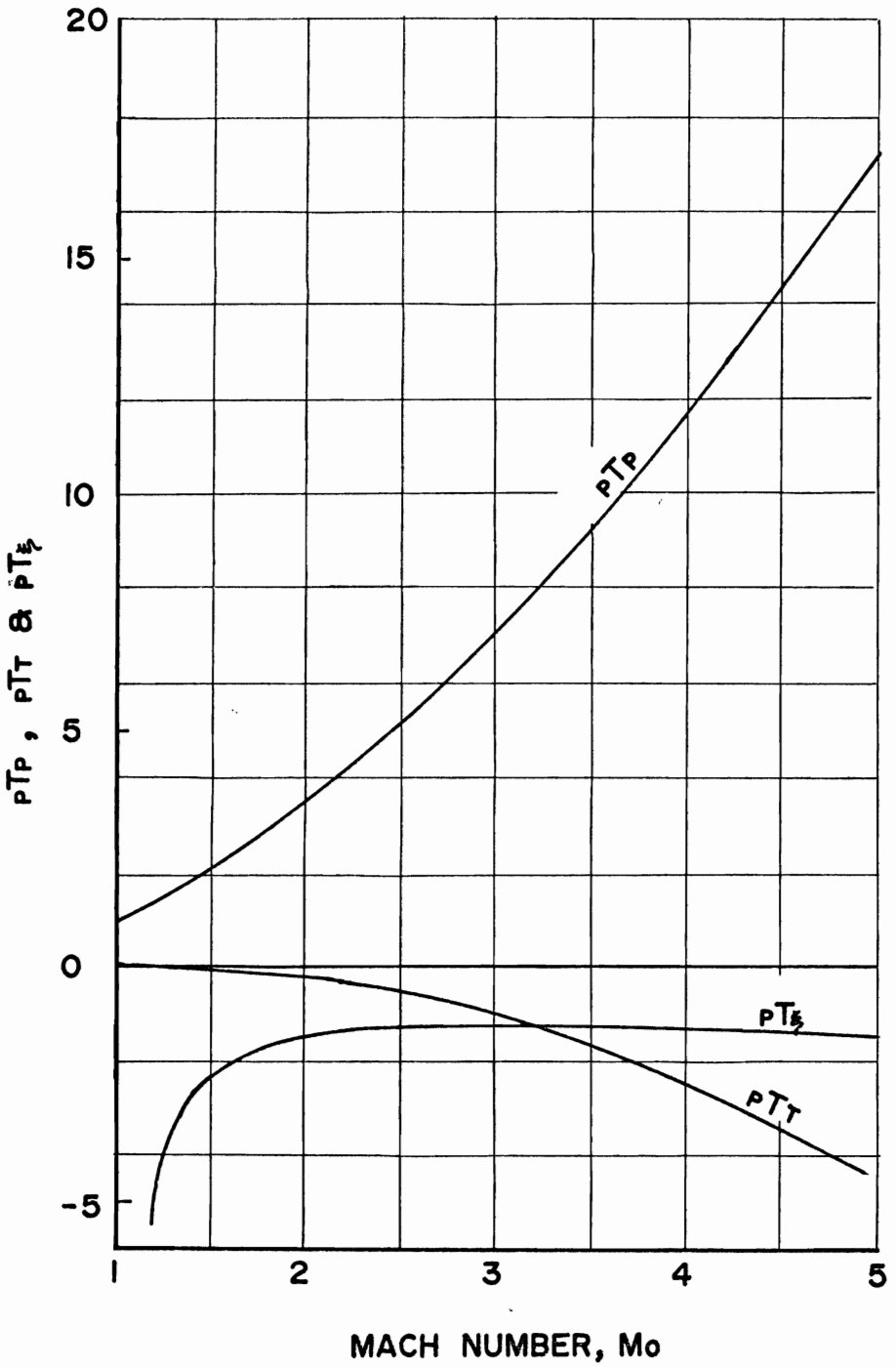

FIG.16 SHOCK WAVE CATCHES UP WITH PRESSURE PULSE (DISTURBANCE IS GENERATED IN THE UPSTREAM OF SHOCK)

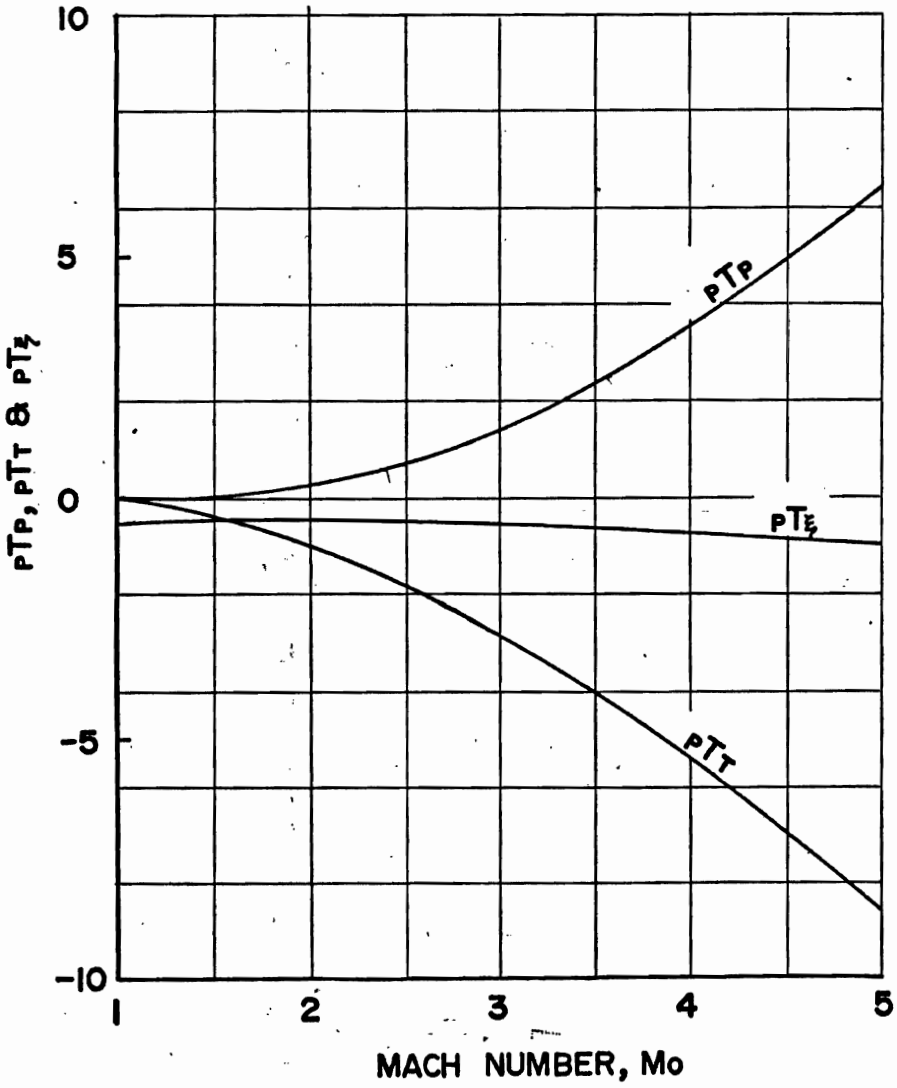

FIG.17 TIME–SPACE DIAGRAM OF SHOCK–DISTURBANCE INTERACTION (DISTURBANCE IS ASSUMED TO BE A COMPRESSION WAVE AND GENERATED IN DOWNSTREAM OF SHOCK)

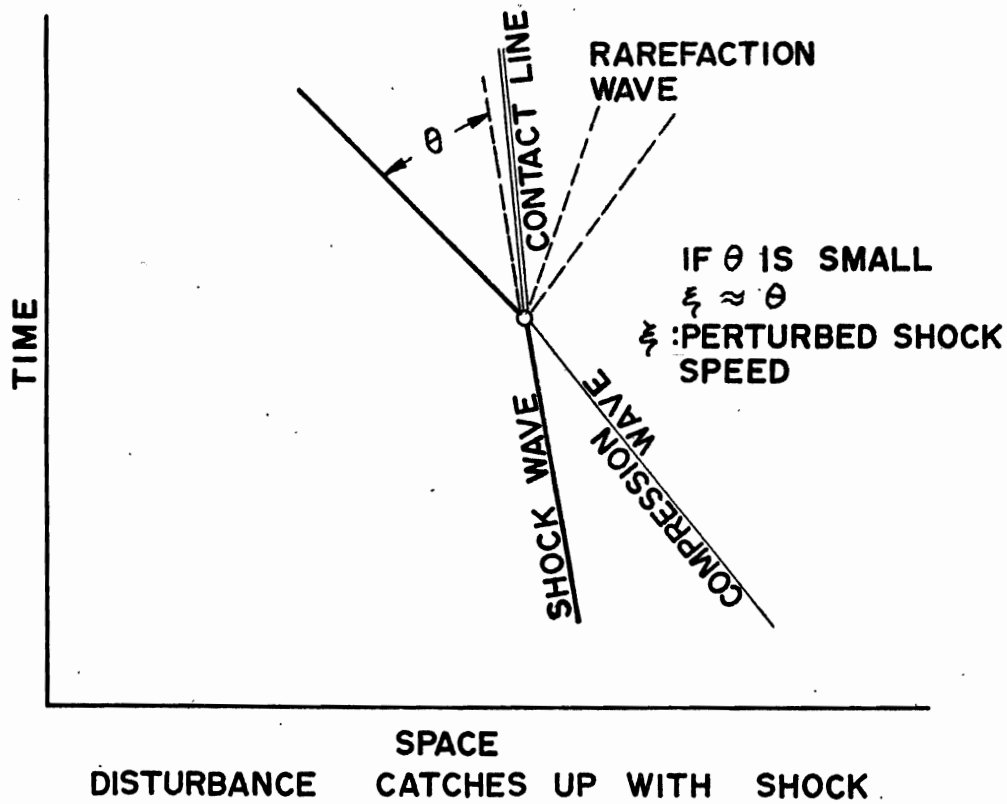

FIG. 18 PRESSURE PULSE CATCHES UP WITH SHOCK WAVE (DISTURBANCE IS GENERATED IN THE DOWNSTREAM OF SHOCK)

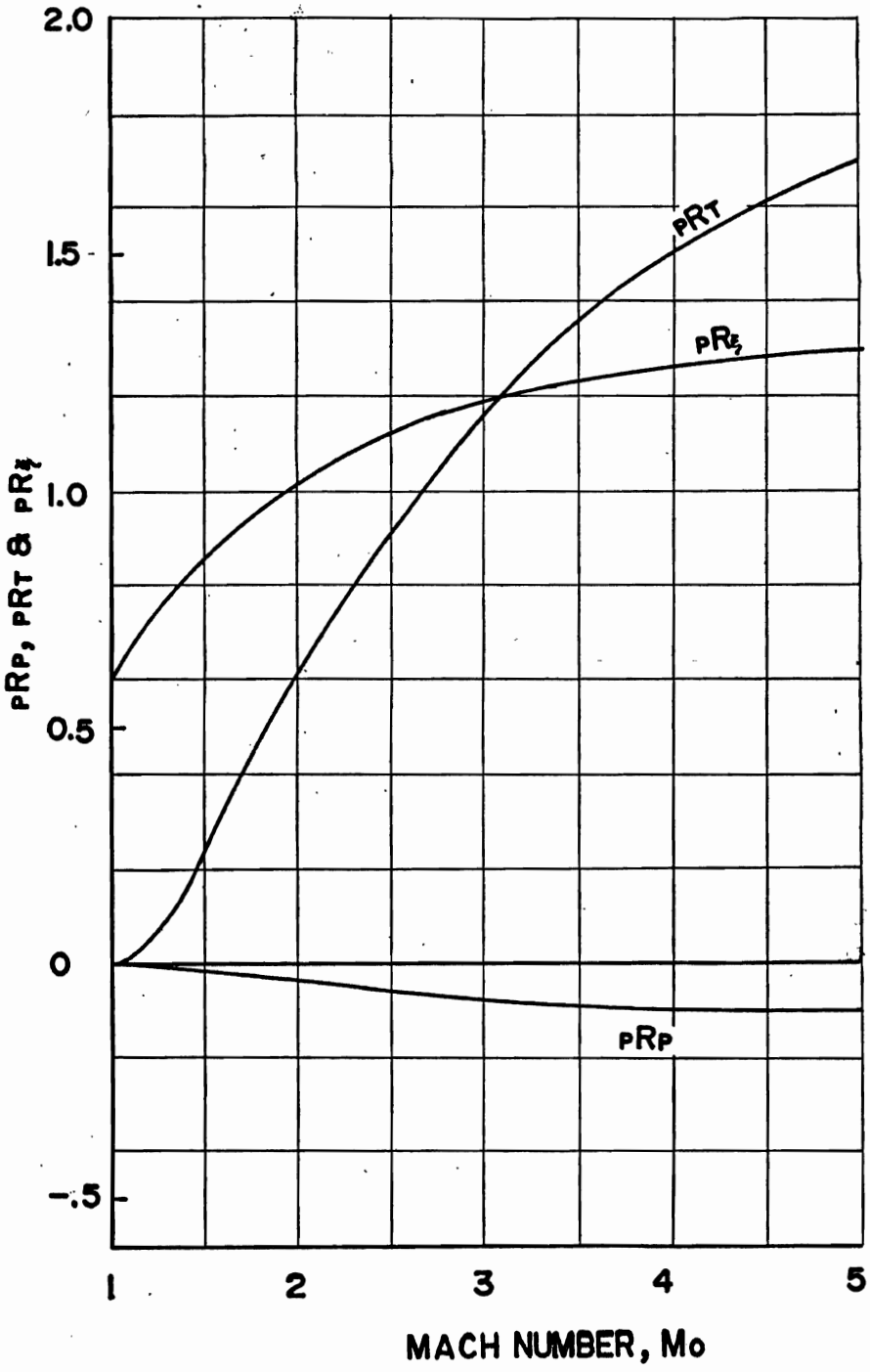

FIG. 19 STAGNATION STREAMLINE DURING BUZZ

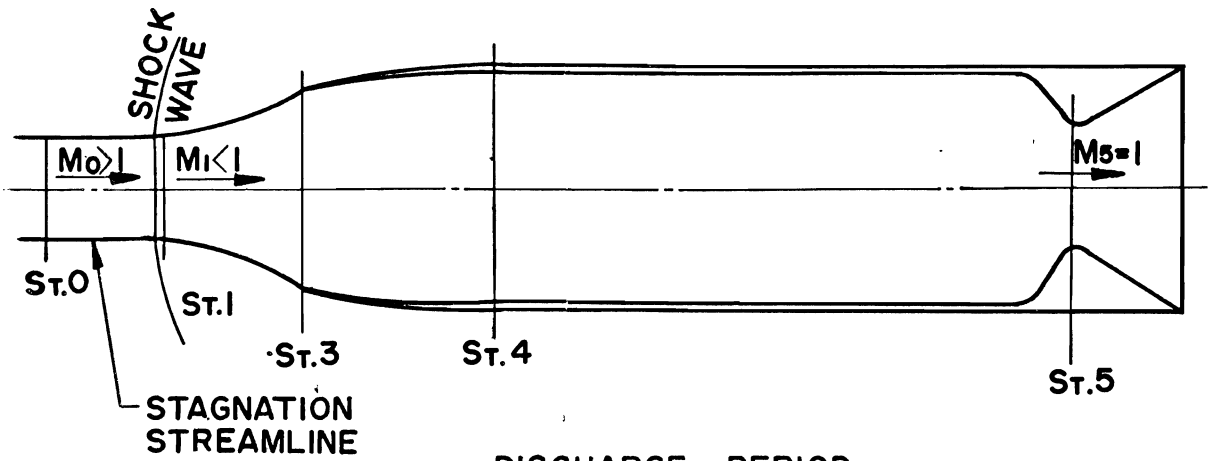

DISCHARGE PERIOD

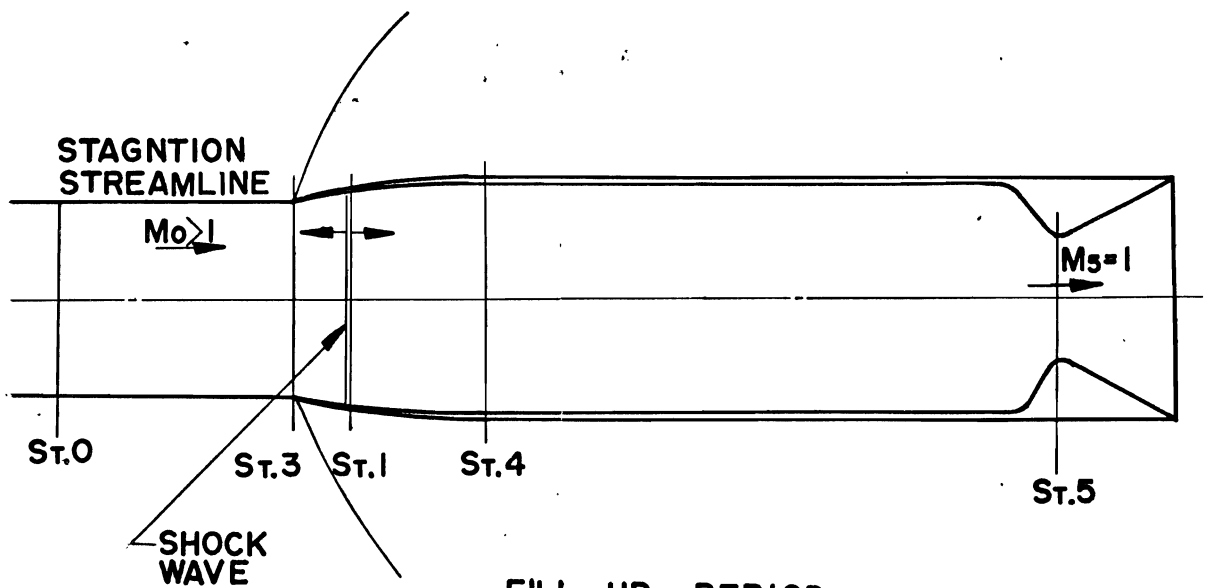

FILL-UP PERIOD

FIG. 20 PRESSURE DROP DURING DISCHARGE PERIOD

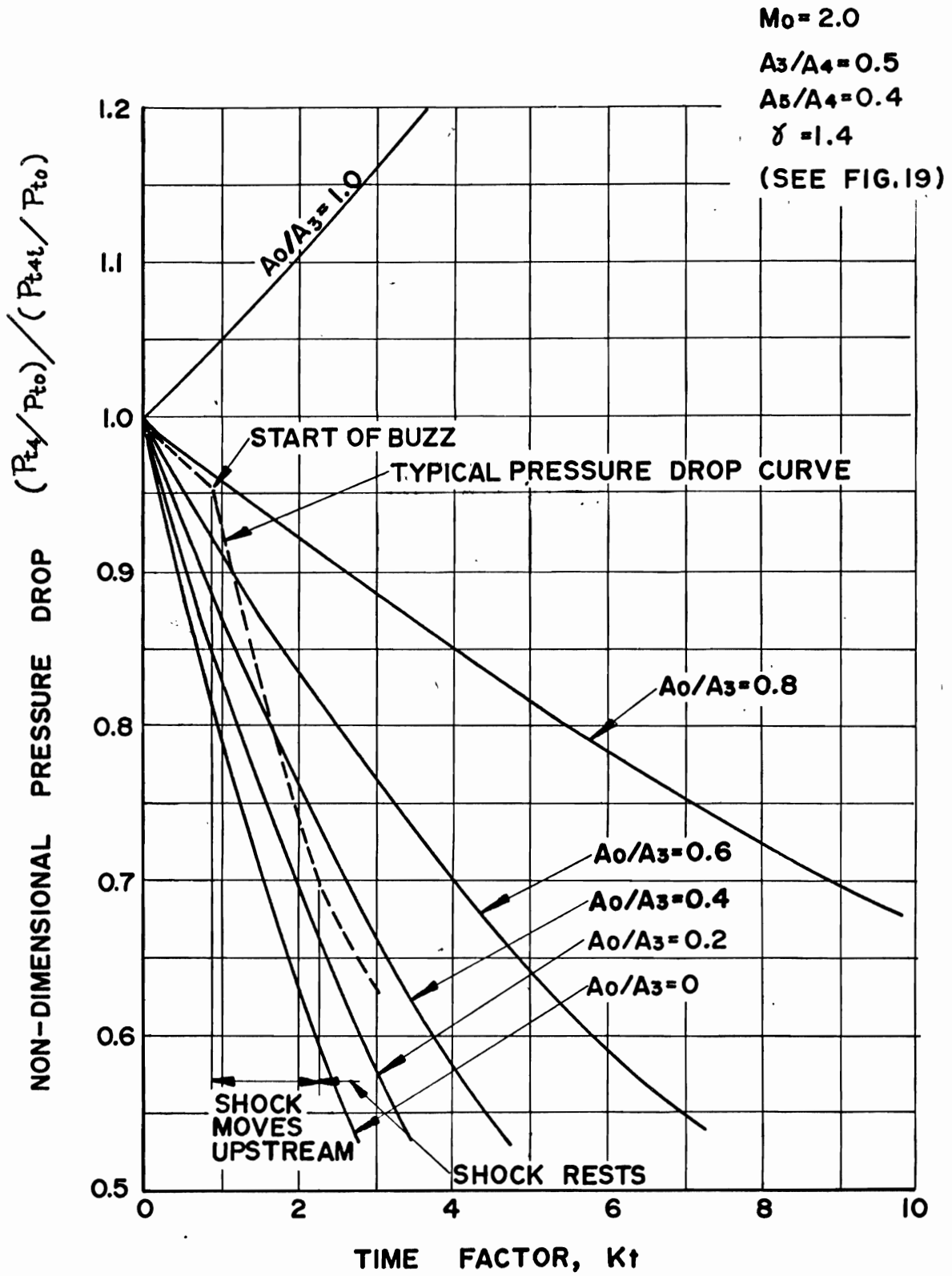

FIG. 21 PRESSURE BUILD UP DURING FILL-UP PERIOD

$M_0 = 2.0$
$A_3/A_4 = 0.5$
$A_5/A_4 = 0.4$
$\gamma = 1.4$
(SEE FIG. 19)

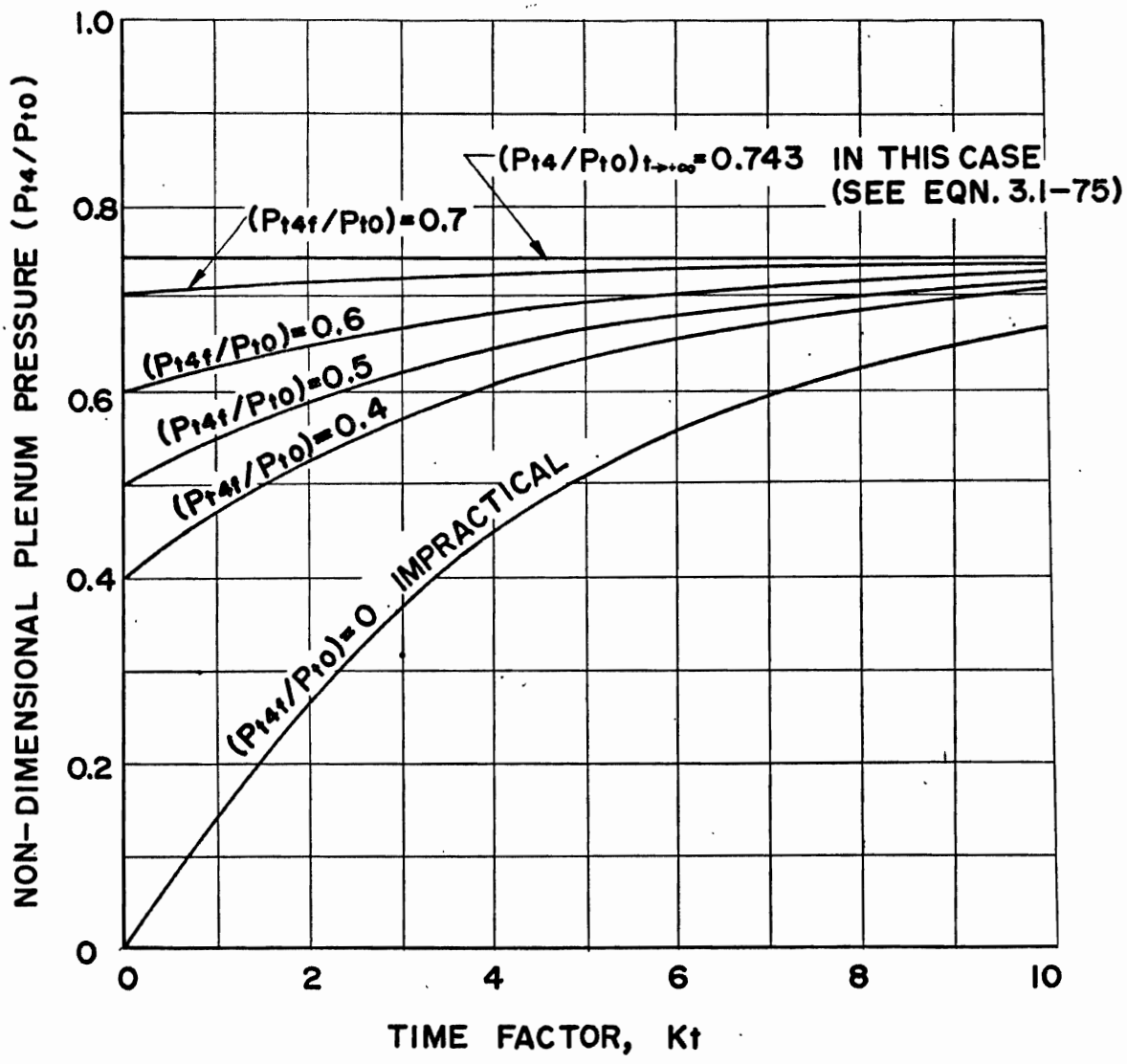

FIG.22 DIFFUSER THROAT MACH NUMBER, M_3, VERSUS INLET LIP MACH NUMBER, M_2

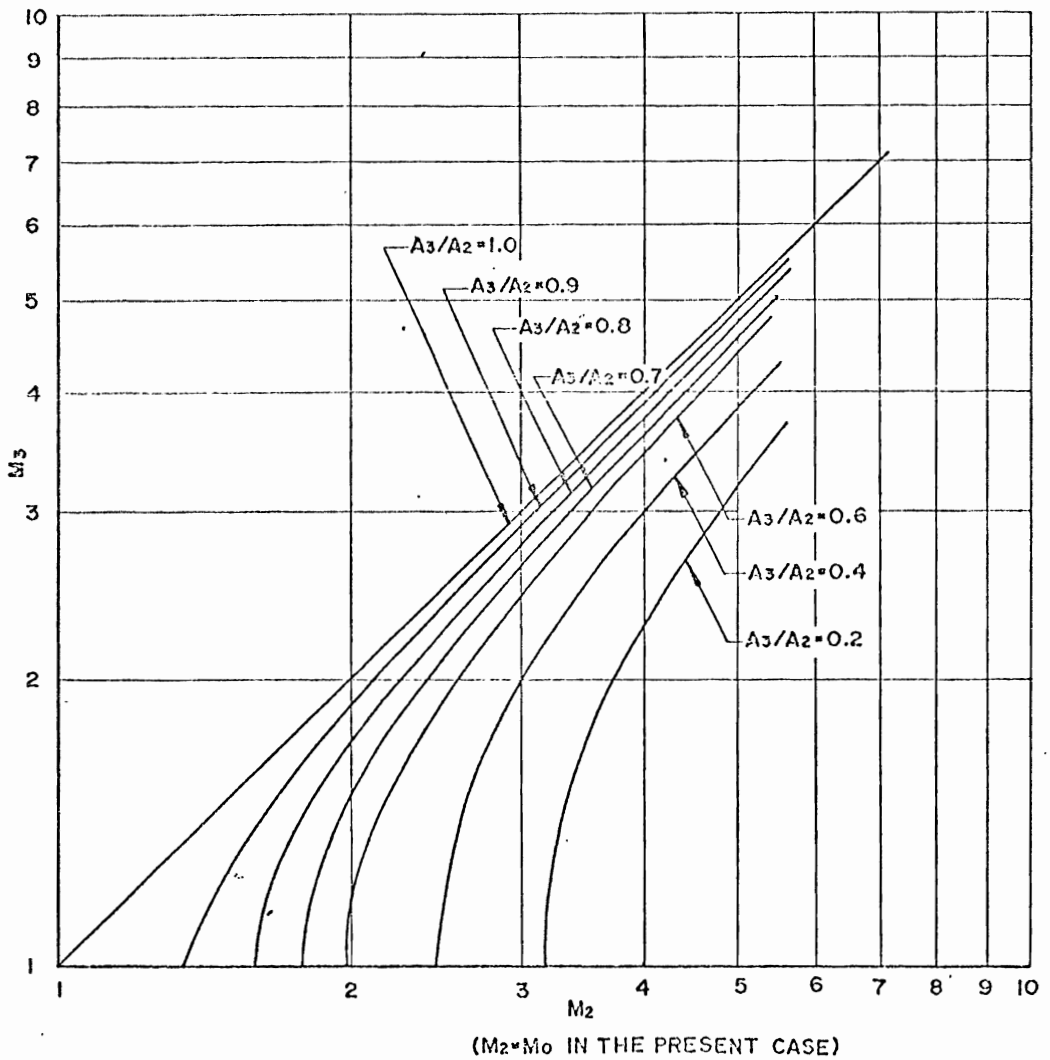

FIG.23 RATE OF PLENUM PRESSURE BUILD-UP (EQN 3.1-79) & (EQN. 3.1-78)

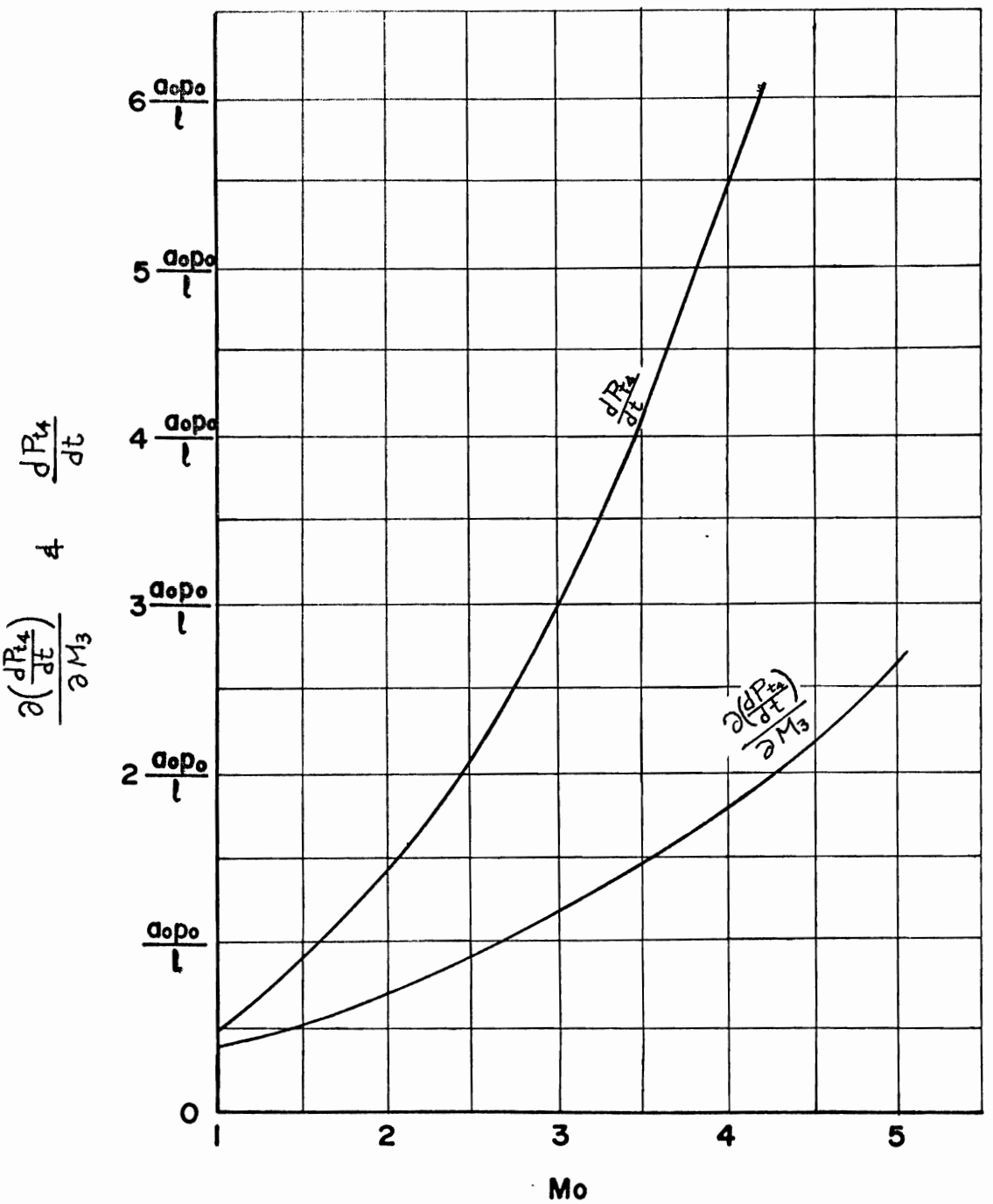

FIG 24 FREQU[illegible]F VERSUS MACH NUMBER

$$f = \frac{2n-1}{4}\frac{a}{l}(1-M_4^2)$$

WHERE $n = 1, 2, 3, \cdots\cdots$

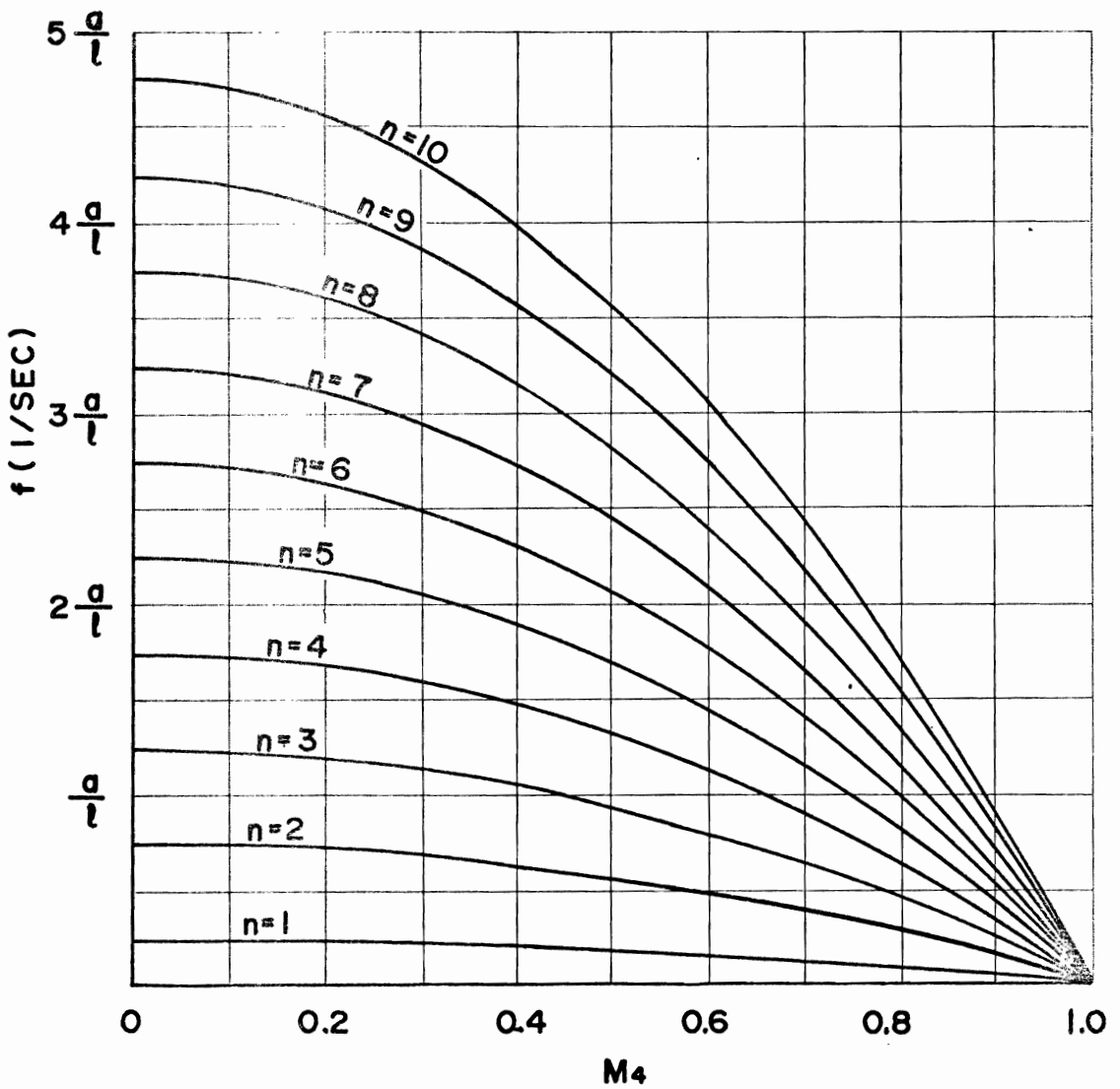

FIG. 25 LOGARITHMIC DECREMENT OF AMPLITUDE VERSUS FLOW MACH NUMBER